UNIVERSITÀ
DEGLI STUDI
DI PADOVA

Sede Amministrativa: Università degli Studi di Padova

Dipartimento di
Medicina Molecolare

CORSO DI DOTTORATO DI RICERCA IN: Medicina Molecolare
CURRICOLO: Medicina Rigenerativa
CICLO: XXX

Role of mitochondrial STAT3 in the metabolism of mouse embryonic stem cells

Tesi redatta con il contributo finanziario di Giovanni Armenise-Harvard Foundation

Coordinatore: Ch.mo Prof. Stefano Piccolo
Supervisore: Prof. Graziano Martello
Co-Supervisore: Dr.ssa Elena Carbognin

Dottorando: Betto Riccardo Massimiliano

INDEX

ABSTRACT

Stat3 is a transcription factor activated by the cytokine LIF (leukemia inhibitory factor) in mouse embryonic stem (ES) cells. The LIF/Stat3 axis maintains ES cell self-renewal through the induction of nuclear target genes such as Klf4 and Tfcp2l1. Here I report that Stat3 has a parallel function as a regulator of mitochondrial activity. Stat3 binds the mitochondrial DNA and increases the transcription of subunits of the respiratory chain, leading to increased respiration and optimal ES cell proliferation. Indeed, deletion of Stat3 results in reduced respiration and proliferation of ES cells. I performed transcriptomic and metabolic profiling to understand how Stat3 affects the metabolism of ES cells. Stat3 -/- cells display decreased ß-oxidation, decreased activity of the Krebs cycle and are more dependent on Glycolysis for proliferation, indicating a profound metabolic rearrangement. Moreover, Stat3-/- cells differentiate faster than wild-type cells, and such effect can be rescued by expression of Stat3 specifically in the mitochondria. In sum, my results show that Stat3 controls the metabolism of murine ES cells and that a balanced metabolic profile is critical for efficient proliferation and differentiation of Pluripotent cells.

Key words:
LIF/Stat3
Embryonic stem cells
Mitochondria
Metabolism

SOMMARIO

Stat3 è un fattore di trascrizione attivato dalla citochina LIF (leukemia inhibitory factor) nelle cellule staminali embrionali murine. La via di segnale di LIF/ Stat3 è in grado di mantenere il self-renewal e la pluripotenza attraverso l'induzione di target nucleari come Klf4 e Tfcp2l1. In questa tesi di Dottorato è riportato che Stat3, in aggiunta alla propria funzione nucleare, regola anche l'attività mitocondriale. Stat3 è in grado di legare il DNA mitocondriale e incrementare la trascrizione delle subunità della catena respiratoria, permettendo l'aumento della respirazione con un conseguente aumento della proliferazione delle cellule embrionali staminali murine. Infatti la delezione del gene Stat3 in queste cellule causa una riduzione sia della respirazione che della proliferazione. Cellule Stat3-/- presentano inoltre una diminuzione della Beta ossidazione degli acidi grassi, ridotta attività del ciclo di Krebs ed una aumentata dipendenza dalla glicolisi per la loro proliferazione, indicando un profondo riassetto metabolico. Inoltre cellule Stat3-/- presentano un'aumentata propensione al differenziamento rispetto a cellule wild-type. Interessante è stato notare che la presenza di Stat3 esclusivamente nel mitocondrio è in grado di ritardare il differenziamento nelle cellule Stat3-/-. Per riassumere, i risultati di questo lavoro mostrano che Stat3 è in grado di controllare il metabolismo delle cellule staminali murine mantenendo un profilo metabolico essenziale per un efficiente proliferazione e differenziazione delle cellule Pluripotenti.

PUBLICATIONS

Carbognin, E.*, **Betto, R.M**.*, Soriano, M.E., Smith, A.G., and Martello, G. (2016). Stat3 promotes mitochondrial transcription and oxidative respiration during maintenance and induction of naive Pluripotency. Embo J. 35, 618–634.

* These authors contributed equally to this work.

The work presented in the first part of this thesis was ideated and coordinated by Elena Carbognin PhD, Riccardo Massimiliano Betto and prof. Graziano Martello. I performed experiments together with Elena Carbognin PhD. Important contributions to our work were given by our collaborators: Prof. Nico Mitro for Mass Spectrometry analysis.

INTRODUCTION

Pluripotent cells in vivo and in vitro

Early mammalian embryos are characterised by the presence of a population of cells with the capacity of giving rise to all differentiated cells of the adult. This propriety is called Pluripotency and first emerges in the epiblast of the pre-implantation blastocyst (Nichols and Smith, 2012).

The pre-implantation epiblast is a cluster of 10-20 unspecialized cells placed between the trophoblast and the hypoblast. The epiblast generates the entire foetus during development, but can also be "captured" and cultured in vitro as Embryonic Stem (ES) cells (Figure 1A).

ES cells display two defining features, the ability to give rise to daughter cells with identical properties (self-renewal) and the capacity to maintain their embryonic differentiation potential. When ES cells are injected into a host blastocyst they are able to colonize it and contribute to embryonic development, giving rise to a "chimeric" animal (Nichols and Smith, 2012) (Figure 1A).

LIF stabilizes the Pluripotent state

ES cells are intrinsically very unstable: when exposed to a neutral environment, devoid of any signal, they spontaneously differentiate (Figure 1B). Indeed, ES cells were firstly derived using a "feeder layer" of embryonic fibroblasts with foetal serum. Leukaemia inhibitory factor (LIF), a cytokine produced by feeders, has been the first factor shown to be able to maintain ES cells in an undifferentiated, Pluripotent state without support of feeders (Smith et al., 1988).

LIF is a ligand of the Jak/Stat signalling pathway and is routinely used in the derivation and culture of mouse ES cells (Smith, 2001). LIF binds its receptor

complex gp130/LIF-R (Yoshida et al., 1994), leading to the activation of Janus-associated kinases (JAKs), which in turn phosphorylate the transcription factor signal transducer and activator of transcription 3 (Stat3). Stat3 proteins are phosphorylated on a single carboxy-terminal tyrosine residue (Y705 in Stat3) by JAKs. Phosphorylated Stat3 can dimerise, enters the nucleus and activates the expression of target genes, such as Kl4 Kruppel-like factor 4 (Klf4), gastrulation brain homeobox 2 (Gbx2) and transcription factor CP2-like 1 (Tfcp2l1) (Martello et al., 2013) (Figure 1C, left panel). Blockade of LIF signal causes ES cell differentiation. Genetic inactivation of Stat3 has the same effect. Finally, over-activation of Stat3, in the absence of LIF, is sufficient to maintain ES cells self-renewal (Niwa et al., 1998). All these results suggest that LIF maintains ES cell self-renewal through Stat3.

2i culture conditions

An alternative culture environment allowing ES cell culture in the absence of LIF has been recently described. Such culture conditions rely on two inhibitors (2i), called Chiron (CH99021) and PD (PD0325901) (Ying et al., 2008).

Chiron is a specific Gsk3 (glycogen synthase kinase-3) inhibitor, which induces estrogen related receptor beta (Esrrb) through de-repression of TCF3 (also known as Tcf7l1) (Martello et al., 2012). Gsk3 is a negative regulator of many biological processes and proteins (Doble and Woodgett, 2003). Still, the effect of Gsk3 inhibition on ES cell self-renewal is mediated primarily by the wingless-type MMTV integration site family (Wnt) pathway.

Wnt signalling starts with the binding of Wnt ligands to the LRP/Frizzled receptor complex on the cell membrane (Figure 1C middle panel). This leads to activation of Dishevelled proteins, which in turn block the ß-catenin destruction complex. The destruction complex is formed by several proteins: Axin, adenomatosis polyposis coli (APC), GSK3 and CK1a. GSK3 promotes the phosphorylation of ß-catenin, leading to its degradation.

ß-catenin can interact with transcription factors of the TCF/LEF family, regulating the expression of target genes. In ES cells, TCF3 is the most expressed TCF/LEF family member and acts as a repressor. When Wnt signal is active, ß-catenin accumulates and blocks TCF3, resulting in de-repression of TCF3 target genes. The GSK3 inhibitor Chiron mimics Wnt activation, by blocking the destruction complex activity. Indeed, Wnt can partially substitute for Gsk3 inhibition and can reduce ESC differentiation (Berge et al., 2011; Yi et al., 2011). Tcf3 is a major negative regulator of ESC self-renewal (Guo et al., 2011; Pereira et al., 2006). Esrrb is a direct target of Tcf3 repression and the main factor mediating the self- renewal response to Gsk3 inhibition (Martello et al., 2012). Esrrb acts independently of LIF/Stat3, conferring flexibility and robustness to naive ESC self-renewal (Figure 1D).

Another important pathway involved in ES cell self-renewal is fibroblast growth factor (FGF) signalling. FGF promotes the differentiation of ES cells, through activation of downstream kinases MEK and ERK (Figure 1C, right panel). Mutant of ERK in ES cells are resistant to differentiation (Kunath et al., 2007). Similarly, chemical inhibition of FGF signal at the level of FGF receptor or MEK delays differentiation (Ying et al., 2008). Nanog is repressed by FGF signalling, probably via ETS proteins, but the molecular mechanism is still unknown. Inhibition of MEK with PD results in increased Nanog expression, that in turn promotes self-renewal and delay differentiation.

The 2 inhibitors in combination are sufficient to culture ES cells in the absence of LIF, and have allowed the derivation of Stat3-/- cells (Ying et al., 2008), proving genetically that 2i does not work through the LIF/Stat pathway. Stat3-/- cells cultured in 2i are morphologically indistinguishable from wild-type ES cells. They show no induction of Stat3 target genes after LIF stimulation and differentiate rapidly when exposed to LIF without 2i, confirming their incompetence to respond to LIF.

Main Pluripotency factors

A Pluripotency factor may be defined as a gene that directly controls Pluripotency in the pre-implantation epiblast or in ES cells. The POU-domain transcription factor Oct4 (Pou5f1) is the first characterized Pluripotency factor (Schöler et al., 1990). In the absence of Oct4, Pluripotent cells do not form in the embryo and ES cells cannot be derived. Inactivation of Oct4 in ES cells causes rapid differentiation in trophoblast cells (Nichols et al., 1998). The SRY-box transcription factor Sox2 is also essential for ES cell self-renewal. Sox2 inactivation in ES cells results in trophoblast formation, phenocopying Oct4 deletion (Masui et al., 2007). Sox2 is an Oct4 partner: it physically interacts with Oct4 protein (Pardo et al., 2010) and binds DNA together with Oct4 at Oct/Sox elements (Chen et al., 2008).

Oct4 and Sox2 are often considered the “core” Pluripotency factors, because they are absolutely required to establish and maintain the Pluripotent state. Interestingly, the core factors are not directly regulated by either LIF/Stat3, Wnt or FGF pathways. Other transcription factors are activated by external signals, which in turn stabilise the expression of Oct4 and Sox2 (Figure 1D).

Mitochondria in Pluripotent Stem cells

Mitochondria have an essential role in energy production through the process of oxidative phosphorylation (OXPHOS), also called mitochondrial respiration. Mitochondria can convert nutrients into adenosine triphosphate (ATP), which is the main “fuel” of the cell. Mitochondria are also implicated in other processes such as production of reactive oxygen species (ROS), pyrimidine and lipid biosynthesis and apoptosis (Figure 2A) (Duchen, 2004).

Each mitochondrion contains 2-10 copies of mitochondrial genomic DNA (mtDNA) (Wiesner et al., 1992). The mtDNA consists of 15-17 kilobases and is

organized as a circular, covalently closed, double-stranded DNA. The mtDNA encodes for 37 genes, 13 are subunits of the respiratory chain (Figure 2C), 22 are transfer RNA (tRNA) and 2 are small and large subunits of ribosomal RNA (rRNA) (Figure 2B) (Ward et al., 1981).

Mouse ES cells are very proliferative (cell cycle length of ~16 hours) and constantly require a high supply of energy. Accordingly, the levels of oxidative phosphorylation observed in ES cells are very elevated, compared to more differentiated cells such as Mouse Embryonic Fibroblasts (Zhou et al., 2012) (Figure 2D).

Little is known about the signals and proteins controlling mitochondrial activity in ES cells. Stat3, the transcription factor downstream of LIF, has been recently shown to localize to the mitochondria and regulate its activity by only partially understood mechanisms (Wegrzyn et al., 2009).

Recent reports showed that Stat3 can localize to the mitochondria of cardio-myocytes, pro-B cells and Ras-transformed cells (Gough et al., 2009; Wegrzyn et al., 2009). This pool of Stat3 can modulate the mitochondrial activity and permeability. Moreover, mitochondrial Stat3 has been shown to be implicated in normal tissues homeostasis and in pathological conditions, such as tumour growth and tissue damage in response to ischemia/reperfusion injury (Garama et al., 2016).

The import of Stat3 from the cytoplasm to the mitochondrion is less understood, some data indicate that Stat3 after PKC-dependent phosphorylation interacts with HSP70 and HSP90 chaperons and this enhances the Stat3 mitochondrial import, through the transporter outer membrane complex (TOM) (Srivastava and DiGiovanni, 2016). There are evidences that the transport of Stat3 to the mitochondrion correlates with a second site of phosphorylation in the Serine 727 (S727) (Gough et al., 2014; Tammineni et al., 2013). Moreover, Stat3 phosphorylation in S727 is associated with an increased activity of Complex I and II (Gough et al., 2009;

Wegrzyn et al., 2009) and its capacity to bind mitochondrial DNA (Szczepanek et al., 2011; 2015).

Based on all these observations, Stat3 represents an ideal candidate as a regulator of OXPHOS in murine ES cells.

Metabolic dynamics of ESCs

Glycolysis is a series of enzymatic reactions that happen in the cytosol that convert Glucose in Lactate (anaerobic) or Pyruvate (aerobic) with a concomitant production of ATP and NADH. Some of the intermediate metabolites of Glycolysis can be diverted to others metabolic pathways.

When oxygen is available, Glycolysis converts Glucose into Pyruvate, which is transferred to the Krebs cycle and converted into Acetyl-CoA. The Krebs cycle oxidizes acetyl-CoA to generate NADH and FADH, an electron carrier that is essential for the function of electron transport chain (ETC). Another important source of Acetyl-CoA and NADH/FADH2 is the ß-oxidation (B-Ox) of fatty acids. The ETC uses the electron carrier to pump proton out of the mitochondrial matrix (Figure 2A, light blue) into the inter-membrane space (dark blue). The ATP synthase generates ATP when the protons flow back. This process is called oxidative phosphorylation (OXPHOS) (Figure 2B) and requires also Oxygen for energy production, therefore it is also known as mitochondrial respiration (Figure 2C).

The metabolic profile of mESCs is defined as bivalent, because they can efficiently perform both Glycolysis and mitochondrial respiration, although their mitochondria are immature (Figure2D). This ensures a high supply of ATP allowing efficient proliferation. Yet, some cells preferentially use only one of these metabolic pathways to maintain their survival and proliferation rate, for instance some cancer cells lines preferentially use Glycolysis for energy production.

Although performing only Glycolysis could be less efficient in terms of ATP production (2 ATP molecules come from Glycolysis compare to 36 ATP

molecules from OXPHOS), Glycolysis can be advantageous for other reasons. Glucose intermediates can be diverted to generate several precursors essential for cell division and survival, such as acetyl-CoA for fatty acids synthesis, non-essential amino acids or ribose for the synthesis of nucleotides (Mathieu and Ruohola-Baker, 2017). Furthermore, another potential benefit of excluding mitochondrial respiration is the decreased ROS production that could negatively affect cell survival (Khacho et al., 2016; Sieber et al., 2016).
When mES differentiate, they transit through a state called primed Pluripotency, because the cells start to express markers of germ layers and are therefore primed for differentiation. Primed Pluripotent cells are only glycolytic (Figure 2D). The same transition from bivalent to glycolytic metabolism is observed also in the embryo and could be justified by the limited availability of Oxygen upon implantation. In other words, primed Pluripotent cells in the embryo change their metabolism to better adapt to the environment and such switch may be important to support the high proliferation rate of mES and their differentiated descendants (Houghton et al., 1996). Interestingly, this strategy is used in high proliferative cancer cells, and it is called Warburg effect (Warburg et al., 1927).

It is not known whether the change in metabolism observed during differentiation of ES cells is simply an adaptive response to the change of environment, or if it plays a functional role during the differentiation process. Is the change in metabolism required for differentiation of ES cells?

AIM OF THE PROJECT

Embryonic Stem cells are derived from early embryos and retain the ability to differentiate into all cell types of the adult, an ability called Pluripotency. Since its discovery in 1987 the cytokine Leukemia Inhibitory Factor (LIF), and its downstream transcription factor Stat3 are key to derive ES cells and maintain them Pluripotent. Recently, a new culture condition based on two inhibitors (2i) allows maintaining mouse ES (mES) cells undifferentiated without LIF. Under 2i culture conditions an ES cell line with a genetic inactivation of Stat3 has been derived. Stat3 -/- cells remain Pluripotent in presence of 2i but display defects in proliferation compare to wild type cells (Ying et al. 2008).

My initial aim was to understand why in the absence of Stat3 proliferation of mES cells is reduced. I observed that in the absence of Stat3 the transcription from mitochondrial genome and respiration were reduced. Recently it has been reported that Stat3 can localize in the mitochondria in different cell types and modulate the mitochondrial activity. Through a series of genetic experiments, I demonstrated that also in mES cells mitochondrial Stat3 is able to regulate the mitochondrial transcription and activity and, consequently the proliferation of mES cells.

A second aim was to understand the global impact of Stat3 on metabolism of ES cells. Murine ES cells are characterized by a bivalent metabolism that guarantees the high production of energy necessary for their rapid proliferation. Mitochondrial Stat3 seems critical to maintain this peculiar metabolic profile, so I wanted to understand what are the effects of Stat3 on critical metabolic pathways. Preliminary results obtained by Mass Spectrometry analysis highlight that mitochondrial Stat3 controls Glucose and fatty acid metabolism and such results have direct implications also for both ES cell proliferation and differentiation.

RESULTS

The LIF/Stat3 axis promotes ES cell proliferation and mitochondrial transcription

The cytokine LIF and its downstream mediator Stat3 have been shown to be critical for self/renewal and maintenance of Pluripotency of mouse Embryonic Stem (ES) cells. Indeed, mouse ES cells are routinely cultured in the presence of LIF and serum/containing media, a condition defined “LIF+Serum” (Smith et al., 1988). It has been previously shown that the main transcriptional targets of the LIF/Stat3 signal are Klf4, Tfcp2l1 and Gbx2, three transcription factors that individually are able to promote self/ renewal of ES cells (Martello et al., 2013).

An alternative culture environment allowing ES cell expansion in the absence of LIF has been recently described. Such culture conditions are serum/free and chemically defined, and rely on two inhibitors (2i) (see Introduction and Figure 2B-C). The 2 inhibitors in combination are sufficient to culture ES cells in the absence of LIF (Ying et al., 2008).

Given that the two inhibitors work on the FGF and WNT pathways, that are not directly related to LIF/Stat3, it should be possible to genetically inactivate Stat3 using 2i conditions. Indeed, Stat3-/- ES cells have been previously derived and characterized in 2i, they maintain the ability to self-renewal and to recolonize the mouse embryo upon blastocyst injection (Martello et al., 2013; Wray and Hartmann, 2012; Ying et al., 2008). Moreover, Stat3-/- cells are a precious tool that allows us to better investigate the effects of LIF/Stat3 in mouse ES cells.

Interestingly, addition of LIF to 2i (“2i+LIF” conditions) has been shown to be

beneficial, resulting in a more robust expansion of ES cells (Figure 3A, compare dark blue lines and light blue lines). Stat3 is considered the main downstream mediator of LIF signalling in ES cells. I observed that LIF had no effect on Stat3-/- cells, suggesting that the positive effect of LIF on proliferation is mediated by Stat3 (Figure 3A, red bars).

Such difference in cell number could also be in part explained by an effect of LIF on cell survival. To measure the percentage of viable cells under the two cultured conditions I used Trypan blue, a dye that specifically stains dead cells. I could not observe any significant difference in the percentage of viable cells (Figure 3B), suggesting that LIF does not affect survival of ES cells.

In order to understand how LIF promotes proliferation of mES cells I analysed the transcriptome of cells cultured in 2i without LIF and with a pulse of LIF for 1h or 24h, by RNA sequencing. The aim was to identify the early transcriptional targets implicated in mES increased proliferation. Unexpectedly most of the identified targets were mitochondrial genes coding for specific subunits of the respiratory chain (Figure 3C and D). I did not observe this up-regulation in mES Stat3-/- mES cells (Figure 3D).

I performed quantitative Real-time PCR (qPCR) to validate our RNA-sequencing results. Cells were either acutely stimulated with LIF or kept in 2i+LIF conditions for 2 passages, to check if the observed transcriptional responses were stable over time. I observed that LIF induces up-regulation of mitochondrial transcripts and that this effect is not transient (Figure 3E, top). Finally, LIF treatment did not induce mitochondrial transcripts in Stat3-/- cells (Figure 3E, bottom) as observed by RNA sequencing.

I then asked whether the up-regulation of mitochondrial transcript could be due to direct regulation of the mitochondrial genome. I generated a reporter construct containing the D- loop, the unique promoter region present in the mitochondrial genome, followed by a minimal promoter and the Firefly luciferase ORF (D-loop-Lux) (Figure 4A). I performed a Luciferase assay in ES

cells and observed that transfection of Stat3 in the presence of LIF resulted in increased reporter activity over the control (Figure 4B). As a positive control, I used p53, a protein that has previously been shown to activate mitochondrial transcription. Transfection of p53 resulted in a very mild activation of the reporter. Overexpression of Stat3 induces the reporter, both in the presence or in absences of LIF. This is likely due to basal activation of the LIF pathway and to high levels of expression obtained by transient transfection. These results suggest that Stat3 is able to directly activate the promoter region of the mitochondrial genome.

Next step was to confirm the capacity of Stat3 to bind the mitochondrial genome and directly regulate mitochondrial transcription. I interrogated available data on chromatin immunoprecipitation followed by sequencing (ChIP-seq) (Sánchez-Castillo et al., 2015). I identified two regions in the D-loop with high Stat3 enrichment (region A and B, in Figure 4C) and a third region where binding of Stat3 was negligible (region C, in Figure 4C). I performed ChIP-qPCR and confirmed binding of Stat3 on regions A and B of the D-loop in mES cells (Figure 4D).

ATAD3 is a protein required for the correct assembly of mitochondrial DNA in a structure called nucleoids and it specifically binds to the D-loop, a unique promoter region present in the mt-DNA (He et al., 2007). If Stat3 is able to bind the mitochondrial genome it should co-localise with ATAD3. Proximity Ligation Assay (PLA) is a technique that detects with high specificity and sensitivity a protein-protein interaction in intact cells. When two proteins are in close proximity they are detected by two antibodies that trigger an enzymatic activity resulting in a single fluorescent dot. Thus, I performed a PLA with Antibody against STAT3 and ATAD3 (Figure 4E). First I checked the background signal of this technique using single antibodies, respectively against STAT3 or ATAD3, and I found that only few dots appeared. Conversely when I performed the PLA with both antibodies, I observed a 3 fold increase in the number of dots compared to background. This confirms that STAT3 and

ATAD3 co-localize in the inner mitochondrial membrane near the mitochondrial DNA.

Collectively, these findings suggest that Stat3 directly induces transcription of the mitochondrial genome, but do not rule out other potential effects of Stat3 on the stability or turnover of mitochondrial transcripts.

Mitochondrial respiration is increased in the presence of LIF

Next, I wondered if the up-regulation of mitochondrial transcripts correlates with enhanced cellular respiration in ES cells. To this aim I quantified the level of respiration by Sea Horse assay. This assay allows to measure the consumption of oxygen in live cells over time and to calculate the oxygen consumption rate (OCR).

I first analysed Stat3-/- and +/+ cells and observed a reduction in the basal respiration levels in absence of Stat3 (compare dark blue and red lines in Figure 5A). Moreover, when I maximized oxygen consumption through an uncoupler of mitochondrial membrane called FCCP (Carbonyl cyanide-*p*-trifluoromethoxyphenylhydrazone), Stat3+/+ cells showed a robust increase in OCR, which was far less pronounced in Stat3-/- cells. Finally, Antimycin treatment is used to block mitochondrial respiration. The residual levels of mitochondria-independent oxygen consumption are similar in the two cell lines.

I then asked whether mitochondrial activity could be modulated by LIF signalling in Stat3+/+ cells. I observed that the presence of LIF significantly enhanced the oxygen consumption levels (compare dark blue and light blue lines in Figure 5B), similarly to what I observed above. Further, I measured the relative change in OCR after FCCP treatment in Stat3+/+ cells and I found a significant increase in maximal capacity of respiration in cells cultured with LIF (Figure 5C).

I concluded that LIF signalling is able to boost mitochondrial respiration and

the presence of Stat3 is instrumental for efficient mitochondrial respiration.

After the previous considerations about the increase in the respiration capacity in cells treated with LIF or Stat3 I checked if this effect can be due to an increased mitochondrial biomass. To do this I measured the protein levels of TOM20 and TIM23, two proteins responsible for the translocation of several substances from the cytosol to mitochondria. Western Blot in Figure 5D shows that in presence or absence of LIF mES have the same quantity of TOM20 and TIM23. These results suggest that LIF or Stat3 do not influence mitochondrial biogenesis.

Moreover, to confirm that LIF or Stat3 are not involved in mitochondrial biogenesis I measured the copy number of mitochondrial genome by PCR (Figure 5E). Specifically, I used three pairs of primers for three subunits of Complex I, encoded only by mitochondrial genome, and a pair of primers that amplify a locus of nuclear genome in Chromosome 3. I performed the PCR on DNA from mES cells cultured with or without LIF for several passages. Results confirmed that the copy numbers of mt-DNA are equal in cells treated with or without LIF.

Mitochondrial respiration determines optimal proliferation

LIF through Stat3 is able to increase the proliferative capacity of mES cells, up-regulates the mitochondrial transcripts and increases the oxygen consumption rate, therefore I decided to verify if these effects are causally linked. In other words, I wanted to know if the increase in mitochondria respiration is instrumental for the enhanced proliferation observed in the presence of LIF. For this reason, I have used a known inhibitor of complex I, Rotenone, that is able to decrease the activity of the respiratory chain. I titrated Rotenone and found that concentrations ranging from 50 to 100nM had no effects on cell survival but are able to decrease the respiration capacity (Figure 6A-B). I then tested the effect on proliferation of ES cells by

plating in presence of different combination of LIF and Rotenone and counting cell numbers after 48h (Figure 6C). LIF increased the number of wild-type cells (Figure 6C, compare 1st and 2nd bar). Rotenone treatment abrogated the effect of LIF (compare the 2nd bar to the 3rd and 4th bars). As expected, Stat3 null cells did not respond to LIF (5th vs 6th bar), but also appeared more sensitive to Rotenone (compare 6th to the 7th and 8th bars), a result in line with their reduced respiratory capacity (Figure 6A).

To prove the correlation between respiration and proliferation and exclude potential off-targets effects of Rotenone I used Antimycin, an inhibitor of Complex III of respiratory chain. I first titrated Antimycin and found doses that did not affect cell survival (200nM, 100nM, 50nM) but impaired the respiration capacity (Figure 6D-E). Then I performed a proliferation assay with the three different low doses, in Stat3+/+ and -/- cells (Figure 6F). The proliferation rate was reduced in Stat3+/+ cells and, in agreement with the previous results, in absence of Stat3 mES proliferation was more affected.

Chemical inhibition of the respiratory chain resulted in impaired proliferation. Such results could be potentially due to off-target effects of the inhibitors used. To rule out this possibility I performed an experiment where the respiratory chain was inhibited at the genetic level. I depleted Ndufs3, a Complex I subunit that has been shown to be required for Complex I assembly and activity (Lapuente-Brun et al., 2013), using two different shRNAs. Ndufs3 knockdown resulted in reduced OCR levels and proliferation in response to LIF (Figure 6G-I), consistent with the inhibitors results.

These results indicate that mitochondrial respiration is instrumental for maximal proliferation of ES cells.

Mitochondrial localization of Stat3 is crucial for LIF effects on proliferation

Correlation between respiration and proliferation seems strictly dependent

on the presence of Stat3 (Figure 3A, 5A). I used Stat3-/- cells to verify the role of Stat3 on proliferation. First, I transfected Stat3-/- cells with a construct containing mouse Stat3 coding sequence under the control of a constitutive promoter. Second, I randomly picked several clones, and selected two clones expressing Stat3 protein only two-fold over the endogenous (Figure 7B). Thus, I monitored the correct functionality of exogenous Stat3 through the expression of a canonical nuclear target Socs3 (Figure 7C). Quantitative PCR in Figure 7C shows that Socs3 is re-expressed in both selected clones transfected with exogenous Stat3. Finally, I performed a proliferation assay in Stat3+/+, -/- cells and both clones transfected with exogenous Stat3 (Figure 7D). Proliferation assay confirms that both clones show a full rescue in the proliferation capacity compare to Stat3+/+ cells confirming that proliferation is strictly correlated with the presence of Stat3.

The effects of LIF signalling on ES cells proliferation and mitochondrial activity are strictly dependent on the presence of Stat3 but less is known about its role in the mitochondria. To better understand the role of Stat3 in the mitochondria I transfected Stat3-/- cells with a construct that allows the localization of Stat3 only in the mitochondria, under the control of a constitutive promoter. This is possible through the fusion of mouse Stat3 coding sequence with the mitochondria localization signal (MLS) derived from human COX8A (MLS Stat3 Figure 7A) (Wegrzyn et al., 2009). Subsequently I randomly picked several clones expressing MLS-Stat3 at similar levels to the endogenous Stat3 in wild-type cells (data not shown).

To confirm the presence in the mitochondria of both endogenous and MLS-Stat3 I performed a mitochondrial fractionation experiment followed by Western blot. Mitochondrial and total fractions were probed with STAT3, TOM20 (mitochondrial marker) and TRIM33 (nuclear marker) (Figure 7E). Results confirm the correct isolation of mitochondrial fractions, indeed 90% of nuclear protein TRIM33 disappear in mitochondrial fraction compare to total cell extract, in contrast TOM20 a mitochondrial marker is mainly detectable in

the mitochondrial fraction. Finally, Stat3 is detectable in the mitochondrial fraction in Stat3+/+ cells and is clearly enriched in two selected MLS-Stat3 clones.

Consequently, I checked the capacity of MLS-Stat3 to control the transcriptional response at the mitochondrial level. I performed a qPCR analysis on Socs3, a well-known nuclear Stat3 target and I observed that it was reduced in Stat3-/- cells and not re-induced upon expression of MLS-Stat3, suggesting that MLS-Stat3 is not able to control nuclear transcription. (Figure 7F, blue bars).

In contrast, all mitochondrial targets were re-induced by MLS-Stat3 expression in Stat3-/-, to levels comparable to Stat3 +/+ cells (Figure 7F, yellow bars). These results suggest that MLS-Stat3 controls expression of mitochondrial transcripts.

To confirm the ability of MLS Stat3 to bind the mitochondrial genome I performed a ChIP-PCR against Stat3 and I found a significant enrichment of MLS-Stat3 on regions A and B of the D-loop of the mitochondrial genome, compared to Stat3-/- cells (Figure 7G, see also Figure 4C).

Subsequently, to prove with an independent experiment the interaction between Stat3 and mitochondrial DNA I performed a Proximity Ligation Assay (PLA) with antibody against Stat3 and ATAD3 a protein essential for the correct assembly of nucleoid. PLA shows that in Stat3+/+ cells and in MLS-Stat3 clones ATAD3 and Stat3 co-localized (Figure 7H, see also Figure 4E).

Finally, I examined the functional impact of MLS-Stat3 on proliferation. Proliferation assay confirmed that all the three MLS-Stat3 clones expanded more rapidly than the Stat3-/- cells, and two of the clones showed a complete rescue in the proliferation rate comparable to Stat3+/+ cells (Figure 7I left panel). They displayed the typical compact morphology of undifferentiated ES cells and colony sizes appear on average larger than Stat3-/- cells (Figure 7I right panel).

I can conclude that Stat3 localized to the mitochondria is able to directly enhance transcription of mitochondrial genes and proliferation in mES cells.

Generation of new MLS-Stat3 clones with a Nuclear export signal (MLS-Stat3-NES)

The experiments described in Figure 7 performed with MLS-Stat3 indicate that mitochondrial Stat3, rather than nuclear Stat3, is important for respiration and proliferation. Yet, MLS-Stat3 showed a very weak activation of nuclear Stat3 targets (below 5% of endogenous levels). I reasoned that such minor nuclear "contamination" could confound the interpretation of our results. Therefore, I generated a second construct of MLS Stat3 that contained a nuclear export signal (NES) at the N-terminal part of Stat3 coding sequence**.** This new construct, called MLS-Stat3-NES guarantees that the nuclear localization of Stat3 is completely abrogated. This system allows us to better investigate the role of Stat3 in the mitochondria.

First, I transfected Stat3-/- cell with the new construct MLS-Stat3-NES and randomly picked several clones. The presence of MLS-Stat3-NES is confirmed by Western Blot (Figure 8A, note the shift in molecular weight due to the tagging). Previous cell fractionation experiments showed that in wild-type ES cells ~40% of Stat3 is localised in the mitochondria (Figure 7E). For this reason, I selected only the clones that showed an amount of STAT3 around ~40% of the levels found in wild-type cells.

Second, I performed a qPCR to measure the expression of Stat3 and its canonical nuclear target Socs3. Quantitative PCR confirmed that MLS Stat3 NES is expressed in both clones, but Socs3 is undetectable as in Stat3-/- cells (Figure 8B).

Simultaneously I verified the correct localization in the Mitochondria of Stat3 by ImmunoFluorescence (IF) of Stat3-/-, +/+ and MLS-Stat3-NES.A stained with antibodies against Stat3 and Atad3. IF showed that Stat3 in MLS-Stat3-

NES clones is not detected in nuclei and co-localizes with Atad3 in the mitochondria (Figure 8C). These results collectively indicate that MLS-Stat3-NES does not localise in the nucleus.

I performed a proliferation assay of Stat3+/+, -/- cells and MLS-Stat3-NES clones cultured for 4 days in presence of 2iLIF and counted every 24 hours. Proliferation assay showed that both MLS-Stat3-NES clones have a partial rescue in the proliferation rate if compared to Stat3-/- cells (Figure 8D), confirming that mitochondrial Stat3 increases the proliferation in mES cells.

Finally, to link the proliferation to the respiration I measured the oxygen consumption rate by Seahorse assay, that showed a rescue in the respiration in two MLS-Stat3-NES clones (Figure 8E) compared to Stat3-/- cells. Mitochondrial Stat3 is able to increase the respiration capacity in mES cells and this, again, confirms the link between respiration and proliferation.

Metabolic effect of Mitochondrial Stat3 in mES cells

Given that Stat3-/- cells show reduced respiratory capacity and proliferation it would be easy to hypothesise that the levels of ATP, the key product of mitochondrial respiration, could be reduced in Stat3-/- cells, and that the lack of ATP causes the impaired proliferation I observed. Surprisingly, when I measured intracellular ATP concentration by mass spectrometry I found it increased in Stat3-/- cells compared to Stat3 +/+ (see below). This unexpected result prompted me to investigate in an unbiased way the impact of Stat3 on metabolism of mES cells. For this purpose, I performed a mass spectrometry analysis associated with gene expression analysis in Stat3 +/+, -/- and MLS-Stat3-NES, to measure respectively the amount of metabolites and the expression level of the enzymes involved in the main metabolic pathways.

Principal Component Analysis of the Mass spectrometry data identified three different groups, that correspond to Stat3+/+, -/- and MLS-Stat3-NES. Interestingly PCA shows that Stat3+/+ and Stat3-/- cells are clearly separated

and MLS-Stat3-NES clones lie in between (Figure 9A). This indicates that mitochondrial Stat3 is able to modulate the metabolism of mESCs.

The Heatmap in Figure 9B shows in detail the abundance of key metabolites in Stat3+/+, -/- and two different MLS-Stat3-NES clones. Unsupervised hierarchical clustering correctly identifies the 3 different cell groups, indicating a significant metabolic difference between the three cell lines.

I focused my attention on the main differences between Stat3+/+ and Stat3-/- ESCs. Volcano plot shows the changes in metabolites abundance. Those that are significantly more abundant in Stat3+/+ are shown as blue dots, those that are more abundant in Stat3-/- cells as red dots (Figure 9C). Most of the medium chain carnitines (partially oxidized) are high in Stat3-/- cells, which indicates that the fatty acid oxidation is impaired (red circle). Conversely, most of the intermediates of Krebs cycle are more abundant in Stat3+/+ cells (blue circle). These results indicate an impaired activity of fatty acid oxidation and Krebs cycle in Stat3-/- cells.

Figure 9D shows the abundance of individual metabolites in Stat3+/+, -/- cells and MLS-Stat3-NES clones. Interestingly, the majority of Krebs cycle's intermediates are less abundant in Stat3-/- cells and in some cases MLS-Stat3-NES can rescue this effect.

Despite the reduction in mitochondrial respiration, Krebs cycle and fatty acid oxidation, Stat3-/- cells show increased levels of ATP (Figure 9C yellow circle). Such results suggest that in the absence of Stat3 the cells reconfigure their metabolism, reducing the production of ATP from fatty acid, using alternative energy sources. Thus, I investigated the expression of enzymes associate with Glycolysis in Stat3+/+, -/- and MLS-Stat3-NES. Heatmap shows expression levels of genes coding for all Glycolysis enzymes (Figure 9E); unsupervised hierarchical clustering correctly identifies the 3 groups of cells. Interestingly, Stat3-/- cell shows increased expression of Glycolysis genes compared to Stat3+/+. Expression of MLS-Stat3-NES leads to a global reduction in Glycolysis

gene expression. This result suggests that Stat3-/- cells boosts Glycolysis as a compensatory measure to maintain ATP level.

So far, our results are consistent and indicate that Stat3-/- should rely more on Glucose metabolism, in particular Glycolysis, for energy production. I tested such hypothesis with a functional assay. Cells were cultured in presence of different doses of 2-Deoxy-Glucose (2-DG), a Glucose analogue that cannot be processed by Phosphoglucoisomerase, it competitively inhibits the production of Glucose-6PO4 from Glucose. After 72h of treatment I counted the number of cells (Figure 9F) and found that low concentrations of 2-DG affect proliferation of Stat3-/- cells, with negligible effects on Stat3+/+ and MLS-Stat3-NES clones. I conclude that Stat3-/- cells rely more on Glucose for their proliferation.

Mitochondrial Stat3 delays exit from naïve Pluripotency

All the previous data demonstrate that Stat3-/- cells shift their metabolism from OXPHOS to Glycolysis. A similar shift has been previously reported during the first days of differentiation of mES cells (Zhang et al., 2016; Zhou et al., 2012). In other words, Stat3-/- cells show metabolic changes that are normally observed during the initial phase of differentiation of wild-type cells. This prompted me to investigate the impact of metabolic profile on ES cell differentiation. Firstly, I wanted to check if under the conditions I used for ES cell culture I could see a shift in the metabolism during differentiation. Stat3+/+ cells were cultured without 2i LIF for 24, 48 hours and I measured their respiratory capacity by Seahorse assay. I observed a reduction both in the basal and maximal levels of respiration during the first 2 days of differentiation (Figure 10A), confirming that during differentiation ES cells change their metabolism.

Inspection of the morphology of Stat3+/+, -/- and MLS-Stat3-NES clones cultured without 2i LIF for 24h showed that Stat3-/- cells starts rapidly to form

less compact colonies, they display cytoplasmic protrusions and start to detach from colonies and move. All these are early signs of differentiation (Figure 10B). Such changes were not observed in MLS-Stat3-NES clones.

Based on such findings, I wanted to test more rigorously if Stat3-/- cells differentiated more rapidly than wild-type cells. Thus, I performed a clonal assay followed by alkaline phosphatase (AP) staining of cells cultured without 2i LIF for 24, 48 and 72hours. This assay allows quantification of the percentage of undifferentiated (AP+) and differentiated (AP-) cells present in the dish during differentiation. In Stat3+/+ cells I observed a significant reduction in the number of AP+ colonies only after 48h (Figure 10C, right), and by 72h hours all colonies were AP-, indicating complete differentiation of the cells. Stat3-/- cells decreased drastically the percentage of AP+ positive colonies after 24h, much faster than Stat3+/+ cells. Notably, expression of Stat3 in the mitochondria is sufficient to delay the differentiation.

An independent way to assess cell differentiation is to measure the expression of early differentiation markers such as LIN28a/b. Quantitative PCR results in Stat3+/+ cells show a slow upregulation of such markers during the first days of differentiation (blue lines in Figure 10D). In Stat3-/- cells the same markers were already more expressed in 2iLIF. Strikingly they were induced more rapidly and robustly during differentiation, while MLS-Stat3-NES clones behaved similarly to Stat3+/+ cells. Taken together these results indicate that mitochondrial Stat3 regulates the process of ES cell differentiation.

MATERIALS & METHODS

Embryonic stem cell culture

ESCs were cultured without feeders on plastic coated with 0.2% gelatine (Sigma, cat. G1890) and replated every 3–4 days at a split ratio of 1:10 following dissociation with Accutase (GE Healthcare, cat. L11-007). Cells were cultured either in serum-free N2B27- based medium (DMEM/F12 and Neurobasal [both Life Technologies] in 1:1 ratio, 0.1 mM 2-mercaptoethanol, 2 mM L-glutamine, 1:200 N2 [Life Technologies], and 1:100 B27 [Life Technologies]) supplemented with small-molecule inhibitors PD (1 μM, PD0325901), CH (3 mM, CHIR99021) from Axon (cat. 1386 and 1408) and LIF (100 units/ml produced in house), or in GMEM (Sigma, cat. G5154) supplemented with 10% FBS (Sigma, cat. F7524), 100 mM 2-mercaptoethanol (Sigma, cat. M7522), 1× MEM non-essential amino acids (Invitrogen, cat. 1140-036), 2mM L-glutamine, 1mM sodium Pyruvate (both from Invitrogen), and 100 units/ml LIF. For DNA transfection, we used Lipofectamine 2000 (Life Technologies, cat. 11668-019) and performed reverse transfection. For one well of a 6-well plate, we used 6 μl of transfection reagent, 2 μg of plasmid DNA, and 300,000 cells in 2 ml of N2B27 medium. The medium was changed after overnight incubation. Stable transgenic ESCs lines expressing Stat3 or MLS-Stat3 were generated by transfecting cells with PiggyBac transposon plasmids CAG-Stat3, CAG-MLS-Stat3 or CAG-MLS-Stat3-NES with piggyBac transposase expression vector pBase. Selection for transgenes was applied, and stable clones were selected in 2iLIF conditions. For LIF induction experiments, ES cells were cultured in 2i without LIF for > 2 passages, plated (8,000 cells/cm^2) in 2i. Twenty-four hours after plating, cells were treated with LIF for the indicated amount of time. For AP staining, cells were fixed with a citrate–acetone–formaldehyde solution and stained using the Alkaline Phosphatase kit (Sigma, cat. 86R-1KT). Plates were scanned using a Nikon

Scanner and scored manually. Stable transgenic ESCs lines expressing ShNDUFS3 were generated by transfecting cells with a linearized plasmid (pLV(shNDUS3)-mcherrry/puro-U6) with restriction enzyme ScaI (0,5µg of DNA in 12well plate), after transfection cells were sorted for the same mean intensity of mCherry fluorescence.

Proliferation assay

Cell proliferation was assessed by plating 15,000 ES cells in 12-well plate in 2 ml of the indicated medium. Cells were counted every 24 h for 4 days. For Rotenone (Sigma, cat. R8875), Antimycin A (Sigma, cat. A8674) treatments, inhibitors were serially diluted in growth media to a final concentration ranging from 200nM to 50nM and added to the cells right after plating. Control ES cells were cultured in standard medium without inhibitors only with vehicle (DMSO or Ethanol). After 48 hours the ES Cells were dissociated with Accutase, and centrifuged at 500rfc for 5 minute. Medium was removed and cells were resuspended in 1 ml of fresh medium and counted using hemocytometer.

RNA-seq data analysis

RNA sequencing data used in this study are described in Martello et al (2013) and are available in the Array Express repository under accession E-MTAB-1796.

Gene expression analysis by quantitative PCR with reverse transcription

Total RNA was isolated using RNeasy kit (QIAGEN), and complementary DNA (cDNA) was made from 1 µg using M-MLV Reverse Transcriptase (Invitrogen) and dN6 primers. For real-time PCR, I used SYBR Green Master mix (Bioline. Cat. BIO-94020). Technical replicates were carried out for all quantitative PCR. An endogenous control (beta-actin) was used to normalize expression.

Luciferase assay

Luciferase reporter plasmid was derived by subcloning of the D-loop promoter region into pGL3-basic luciferase plasmid (Addgene). CMV-lacZ has been previously described in (Lukas et al., 1997). ES cells were plated in a 12-well plate and transiently transfected with luciferase reporter plasmid with CMV-lacZ to normalize for transfection efficiency (based on CPRG (Merck) colorimetric assay), together with plasmids encoding for the indicated proteins. I transfected 1.5 μg of DNA in each sample by adding the pKS Bluescript plasmid when needed. 48 hours after transfection, the cells were harvested in Luc lysis buffer (25 mM Tris pH 7.8, 2.5 mM EDTA, 10% glycerol, 1% NP-40). Luciferase activity was determined in a Tecan plate luminometer with freshly reconstituted assay reagent (0.5 mM D-luciferin, 20 mM tricine, 1 mM $(MgCO_3)_4$ $Mg(OH)_2$, 2.7 mM $MgSO_4$, 0.1 mM EDTA, 33 mM DTT, 0.27 mM CoA, 0.53 mM ATP).

Chromatin immunoprecipitation (ChIP)

For ChIP experiments, cells were crosslinked, lyzed, and sonicated as described in (Enzo et al., 2015). For immunoprecipitation, sheared chromatin from 5×10^6 cells was incubated overnight at 4°C with 3 lg of rabbit monoclonal anti-Stat3 (Santa Cruz Biotechnologies, cat. sc-482) or with control rabbit IgG. Protein A Dynabeads (Life Technologies) were added for 3 hours after extensive blocking in 0.5% BSA. Washing, de-crosslinking, and DNA purification were performed as in Enzo et al (2015). Results were analyzed by qPCR. Since the D-loop region is partially duplicated in the nuclear genome, I designed primers specific for the mitochondrial genome (see Table 1).

Proximity ligation assay (PLA)

Proximity ligation assay was performed after an overnight incubation with primary antibodies following the manufacturer's instructions (OLink Bioscience). Images were acquired with a Leica SP5 confocal microscope equipped with a CCD camera. Images acquired were analyzed using a custom macro for ImageJ, allowing automated and unbiased analysis.

Oxygen consumption assay

Oxygen consumption was measured using the Seahorse XF24 (Sea- horse Bioscience). For this, ~20 hours before the analysis Stat3+/+, Stat3-/- cells or MLS-Stat3 clones were seeded in a 24-well cell culture plate (Seahorse Bioscience) coated with laminin (Sigma, cat. L2020) at a density of 140,000 cells per well in N2B27 media supplemented with 2i or 2i + LIF (as indicated). It is crucial to have an evenly plated mono-layer of cells to obtain reliable measurements. Cells were maintained in a 5% CO_2 incubator at 37°C, and 1 hours before the experiment, the cells were washed and incubated in 600 µl of DMEM containing 10 mM Glucose (DMEM-high Glucose) pH 7.4 at 37°C in a non-CO_2 incubator. During the experiment, oxygen concentration was measured over time periods of 2 min at 5 minnutes intervals, consisting of a 3-min mixing period and 2 minutes waiting period. Measurements of OCR in basal conditions were used to calculate the basal mitochondrial respiration. After this, the mitochondrial uncoupler FCCP (carbonyl cyanide-p-trifluoromethoxyphenylhydrazone) was added into the media at a final concentration of 200 nM. Oxygen consumption during this phase reflects the maximal mitochondrial respiratory capacity. Finally, ETC activity was blocked by the addition of Rotenone or Antimycin A, both at a final concentration of 200 nM. As a result, OCR drops dramatically, and the oxygen consumed in this situation by the cells comes from a non-mitochondrial origin.

To preform this assay in mES cells during the differentiation process, I plated Stat3+/+ cells 72 hours before the analysis in a 24 wells culture plate at the density of 10,000 cells per well in N2B27 media supplemented with 2iLIF. Only after 24 hours and 48 hours I change the medium and cultured cells without 2iLIF.

Western blot

Cells were washed in PBS and harvested with lysis buffer (50mM Hepes pH 7.8, 200mM NaCl, 5mM EDTA, 1% NP40, 5% glycerol). In order to obtain protein lysates, extracts were exposed to ultrasound in a sonicator

(Diagenode Bioruptor). Cellular extracts were centrifuged for 10 minutes at 4°C to remove the insoluble fraction and total protein content was determined by Bradford quantification, preparing a calibration line using different BSA concentrations. Samples were boiled at 95°C for 5 minutes in 1X Sample Buffer (50mM Tris HCl pH 6.8, 2% SDS, 0.1% Bromophenol Blue, 10% glycerol, 2% 2-mercaptoethanol).

Each sample was loaded in a commercial 4-12% MOPS acrylamide gel (Life Technologies; BG04125BOX/BG00105BOX) and electrophoretically transferred on a PVDF membrane (Millipore; IPFL00010) in a Transfer solution (50mM Tris, 40mM glycine, 20% methanol, 0.04% SDS). Membranes were then saturated with 5% Non-Fat Dry Milk powder (BioRad; 170-6405-MSDS) in TBSt (8g NaCl, 2.4g Tris, 0.1% Tween20/liter, pH 7.5) for 1 hour at room temperature and incubated overnight at 4 °C with the primary antibody diluted in a range of 0,1-0,5% milk powder (depending on antibody) in TBSt. Membranes were then incubated with secondary antibodies conjugated with a peroxidase, diluted in 0,1% or 0,5% milk in TBSt. Pico SuperSignal West chemiluminescent reagent (Thermo Scientific; 34078) was used to incubate membranes and chemiluminescence from the interaction between peroxidase and substrate present in the commercial reagent was digitally acquired by ImageQuant LAS 4000. For antibodies used, see Table 2.

Flow Cytometry

After treatment with Accutase (GE Healthcare, cat. L11-007), live ES cells were dissociated and resuspended in PBS. It is critical to obtain single cell suspensions for optimal staining of samples and to avoid clogging of the injection needle and tubing by cell aggregates. Flow cytometry analyses were performed using a cytometer BD FACSCanto^{TM} with BD FACSDiva^{TM}software.

Propidium iodide/annexin V staining

ES cells were cultured without feeders on plastic coated with 0.2% gelatine; 60,000 ES cells were plated for each well of a 12/well plate in 2 ml of the indicated medium (either LIF+Serum or 2i+LIF, see above the recipes).

Rotenone and Antimycin were serially diluted in growth media to a final concentration ranging from 200nM to 50nM and added to the cells right after plating. Control ES cells were cultured in standard medium without Rotenone or Antimycin with DMSO (vehicle).

For Annexin/V and PI staining I used a commercial kit (Ebioscience, ref. 88/8007/72) following the instructions provided. Briefly, Binding Buffer (4x) was diluted in distilled water (50 ml binding buffer and 150 ml distilled water). After treatment with Accutase, live ES cells were centrifuged at 500 rcf for 5 minute and the medium was removed; cells were washed twice with PBS and resuspend in 195µl Binding Buffer (cell density should be $2/5x10^5$/ml). 5µl Annexin V was added to the cell suspension and incubated for 10 min at room temperature. After this step samples were centrifuged at 500 rcf for 5 minute and supernatant was removed. Cells were washed in 200µl Binding Buffer (1x) centrifuged at 500 rcf for 5 minute and supernatant was remove. Samples were resuspended in 190µl Binding buffer (1x) and 10µl Propidium Iodide (20 µg/ml) were added. Finally, samples were analyzed by flow cytometry using a cytometer BD FACSCanto^{TM} with BD FACSDiva^{TM} software. Each experiment was performed three times, with three technical replicates for each sample.

Mitochondria isolation

Mitochondria isolation was performed from 4×10^7 cells pellet as previously described in (Frezza et al., 2007).

Immunofluorescence

For immunofluorescence, cells were fixed for 10 minutes in cold methanol at 20°C, washed in TBS, permeabilized for 10 minutes with TBST + 0.3% Triton X-

100 at RT (Room Temperature), and blocked for 45 minutes in TBS + 3% goat serum at RT. The cells were incubated overnight at 4°C with primary antibodies. After washing with TBS, cells were incubated with secondary antibodies (Alexa, Life Technologies) for 30 min at RT. For antibodies used, see Table 2.

Cells were mounted with ProLong Gold Antifade Mountant with DAPI (Life Technologies, cat. P36941). Images were acquired with a Leica SP2 confocal microscope equipped with a CCD camera. I quantified the degree of co-localization between different proteins by calculating the Pearson's coefficient R by using the "coloc2" function of the freely available software Fiji (http://fiji.sc/Fiji)

Mass Spectrometry

Cells were grown in 6-well plates, harvested in ice-cold PBS and centrifuged at 2,500g for 3 minutes at 4°C. Pellets were then resuspended in 250µl methanol/acetonitrile 1:1 containing [U-13C6]-Glucose-1ng/µl (internal standard, Sigma Aldrich, 389374) and centrifuged at 20,000g for 5 minutes at 4°C. Supernatant were then passed through a regenerated cellulose filter, dried and resuspended in 100µl of MeOH for subsequent analysis. Amino acids quantification was performed through previous derivatization.

Briefly, 50µl of 5% phenyl isothiocyanate (PITC) in 31.5% EtOH and 31.5% pyridine in water were added to 10µl of each sample. Mixtures were then incubated with PITC solution for 20 minutes at RT, dried under N2 flow and suspended in 100µl of 5mM ammonium acetate in MeOH/H2O 1:1.

Cardiolipin species were extracted from isolated mitochondria using Folch method. After centrifuging for 3 minutes at 20,000g at 4°C, samples were dried under nitrogen flux, resuspended in 200µl of MeOH and passed through a regenerated cellulose filter. Then, samples were dried again and resuspended in 100µl of MeOH for subsequent analyses. Metabolomic data were performed on an API-4000 triple quadrupole mass spectrometer (AB

Sciex) coupled with a HPLC system (Agilent) and CTC PAL HTS autosampler (PAL System). The identity of all metabolites was confirmed using pure standards.

Quantification of different metabolites was performed with a liquid chromatography/tandem mass spectrometry (LC-MS/MS) method using a C18 column (Biocrates) for amino acids and cyano-phase LUNA column (50mm x 4.6mm, 5µm; Phenomenex). Methanolic samples were analysed by a 10 minutes run in positive (amino acids) and 5 minutes run in negative (all other metabolites) ion mode with a 20-multiple reaction monitoring (MRM) transition in positive ion mode and 30 MRM transition in negative ion mode, respectively. The mobile phases for positive ion mode analysis (amino acids) were phase A: 0.2% formic acid in water and phase B: 0.2% formic acid in acetonitrile. The gradient was T0 100%A, T5.5 minutes. 5%A, T7 minutes 100%A with a flow rate of 500µl/min. The mobile phase for negative ion mode analysis (all other metabolites) was phase A: 5 mM ammonium acetate pH 7.00 in MeOH. The gradient was 100%A for all the analysis with a flow rate of 500µl/min. MultiQuant™ software (version 3.0.2) was used for data analysis and peak review of chromatograms. Quantitative evaluation of all metabolites was performed based on calibration curves with pure standards, then data were normalized on micrograms of total protein.

Microarray

Microarray analysis of Stat3+/+, -/- and MLS-Stat3-NES were performed with Illumina Hiscan with the support MouseRef-8 v2.0 Expression BeadChip. Cells are cultured in N2B27 supplement with 2iLIF.

Differentiation

Cells were cultured with or without 2i LIF for 24, 48 and 72 hours. After 72hours cells were detached and replated at clonal density in 2iLIF. Cells surplus are conserved for gene expression analysis. Finally, cells were stained with Alkaline phosphatase after 5 days to evaluate the number of Pluripotent

cells. For AP staining, cells were fixed with a citrate–acetone– formaldehyde solution and stained using the Alkaline Phosphatase kit (Sigma, cat. 86R-1KT). Plates were scanned using a Nikon Scanner and scored manually

Table 1

Gene	Forward primer sequence	Reverse primer sequence
mNd1	CCATTCTAATCGCCATAGCC	ATGCCGTATGGACCAACAAT
mNd4	CGCCTACTCCTCAGTTAGCC	GTGAGGCCATGTGCGATTAT
mNd4l	CTCCAACTCCATAAGCTCCA	GGCTGCGAAAACTAAGATGG
mCo3	TAACCCTTGGCCTACTCACC	ATAGGAGTGTGGTGGCCTTG
mSocs3	ATTTCGCTTCGGGACTAGC	AACTTGCTGTGGGTGACCAT
mStat3	TGTTGGAGCAGCATCTTCAG	GAGGTTCTCCACCACCTTCA
mNdufS3	TTATGGCTTCGAGGGACATC	ATTCTTGTGCCAGCTCCACT
mbactin	CTAAGGCCAACCGTGAAAAG	ACCAGAGGGCATACAGGGACA
Chip A	CATTAAACTATTTTCCCCAAGCA	CAAATGGGGAAGGGGATAGT
Chip B	AAATGCGTTATCGCCCATAC	TCTTCACCGTAGGTGCGTCT
Chip C	TAGTCCGCAAAACCCAATCA	TTGATCAGGACATAGGGTTTGA

Table 2

Antibody	Species	Source	Dilution
Anti-STAT3	Mouse monoclonal	Cell Signalling cat. 9139	WB: 1:1,000 IF: 1:100
anti-TOM20	Rabbit polyclonal	Santa Cruz Biotechnologies cat. 11415	WB: 1:2,000
anti-TIMM23	Mouse monoclonal	BD Biosciences cat. 611223	WB: 1:1,000
anti-TRIM33	Mouse monoclonal	Santa Cruz Biotechnologies cat. 101179	WB: 1:1,000
anti-Atad3A	Rabbit monoclonal	AB-Biotechnologies cat. 224485	IF 1:100
anti-GAPDH	Mouse monoclonal	Millipore cat. MAB374	WB: 1:1,000

Table 3

shRNA	Sequence
ShNDUFS3-1	GGATCACACCAATGCACAATTC
ShNDUFS3-2	CTGACACCCATTGACTCTATA

DISCUSSION

Our results show that LIF through Stat3 is able to increase proliferation operating directly at mitochondrial level. Indeed, in ES cells LIF via Stat3 induces expression of mitochondrial genes encoding components of the respiratory chain. In so doing, LIF/Stat3 pathway enhances oxidative phosphorylation. Interestingly, these effects are not associated with the canonical characterized nuclear LIF/Stat3 target genes (Figure 10E).

Others recent study showed that Stat3 can localize in the mitochondria and modulate the respiration activity of different types of cells (Carbognin et al., 2016; Meier and Larner, 2014; Wegrzyn et al., 2009). Mitochondrial Stat3 has a role in the regulation of the permeability transition pore and interacts with Complex I and II enhancing their activity. Finally, it has recently been reported that Stat3 protein directly binds the mt-DNA and modulates mitochondrial transcription in keratinocytes (Macias et al., 2014).

In my thesis, I elucidated the role of mitochondrial Stat3 in mES cells taking advantage of a construct that allows the expression of Stat3 only in the mitochondria. Expression of this construct in Stat3 null cells led to a rescue in the proliferation and respiration capacity and this confirms that mitochondrial Stat3 controls mES cell proliferation by activating mitochondrial respiration.

It has been previously shown that mES cells are highly proliferative and require a constant and elevated supply of energy. Our initial working hypothesis was that in presence of LIF/Stat3, mitochondria are more active, more energy is available for biosynthesis and cells proliferate more. Surprisingly, when I measured ATP levels I could not observe a reduction of ATP in Stat3-/- cells compared to Stat3+/+ cells. In fact, Stat3-/- cells showed significantly elevated levels of ATP (Fig.9C yellow circle). These results open more questions about the decreased capacity of proliferation in Stat3-/- cells.

To better understand the mechanisms involved in this process I performed a gene expression analysis and a metabolic profiling in Stat3-/- and +/+ cells cultured in presence of LIF. Results display that in absence of Stat3 not only OXPHOS, but also the Krebs cycle and fatty acid oxidation are less active. Consequently Stat3-/- cells boost the Glycolysis pathway to compensate for the reduced activity of the other main metabolic pathways. Interestingly, this strategy is used in high proliferative cancer cells, and it is called Warburg effect (Warburg et al., 1927). It is still not clear why ATP levels increased in Stat3-/-. One possibility is that the reduced cell proliferation of Stat3-/- cells is due to shortage of some amino acids or nucleotides, therefore cells slow down their proliferation and use less ATP. In other words, the increase in ATP levels could be simply due to reduced consumption. I am currently testing this hypothesis by performing a flux analysis whereby Glucose containing a Carbon isotope is administered to ES cells and the levels of unmarked and marked ATP are measured at different times. This experiment will help distinguish between increased production or reduced consumption of ATP in Stat3-/- cells.

It is known that during differentiation mES change dramatically their metabolism and switch from a bivalent to a glycolytic metabolism, specifically during the initial phases of differentiation, when cells start to express markers of the different germ layers and are primed for differentiation (Figure 2D). The same transition from bivalent to glycolytic metabolism is observed also in the embryo and could be justified by the limited availability of Oxygen upon implantation. Stat3-/- cells display a hybrid metabolism between mES cells and Primed cells. Therefore, I performed an assay to measure the propensity to differentiate of mES cells. Results confirmed that Stat3-/- cells differentiate faster than controls, and the expression of mitochondrial Stat3 rescues such effects (Figure 10 C, D).

I put forward a model whereby Stat3-/- cells are more prone to differentiate, because of their unbalanced metabolic profile (Figure 10F). Interestingly, such

findings indicate that metabolism has an active role in the differentiation process instead of being a consequence of it.

Future studies will be needed to better understand the causal relationship between metabolism and the process of differentiation, with the aim of dissecting the molecular mechanism behind such effects.

What are the metabolites responsible for such effects? How is nuclear gene transcription of differentiation markers affected by metabolites?

Several recent studies have highlighted the potential crosstalk between metabolism and epigenetic modifications in Pluripotent cells (Carey et al., 2015; Lu and Thompson, 2012). The action of LIF/Stat3 on mitochondria may therefore be important not only to fulfil a bioenergetics requirement, but to increase the production of cofactors for epigenetic processes, such as demethylation of DNA and histone modification.

FIGURES LEGENDS

FIGURE 1

A) Mouse blastocyst at E3.5 (top left panel). Pluripotent Epiblast cells are highlighted in green. They are the source of ES cells. ES cells derived from the Epiblast and cultured in vitro in presence of the correct signalling environment (top right panel). Chimeric mouse derived after injection of ES cells into a host blastocyst (left bottom panel).

B) Morphology of ES cells cultured with Serum alone (top panel), in Serum with LIF (middle panel) or 2i plus LIF (bottom panel) for 3 days. In the presence of LIF colonies show a uniform edge with no signs of differentiation. Without LIF cells are very heterogenous and differentiated but the combination of LIF with the two inhibitors (Chiron and PD) shows the best uniformed and undifferentiated morphology.

C) Pathway activated by LIF, WNT and FGF with their principal mediators and transcriptional targets (see introduction). Highlighted In blue are the small molecules used to culture ES cells (see Introduction).

D) Schematic diagram of the network of transcription factors controlling Pluripotency. The "core" factors Oct4 and Sox2 are absolutely required for Pluripotency. External signals, such as LIF/Stat3 induce several target proteins which in turn stabilize the network. The targets of the two inhibitors (Chiron and PD) are also highlighted. (Martello et al. 2013)

FIGURE 1 intro

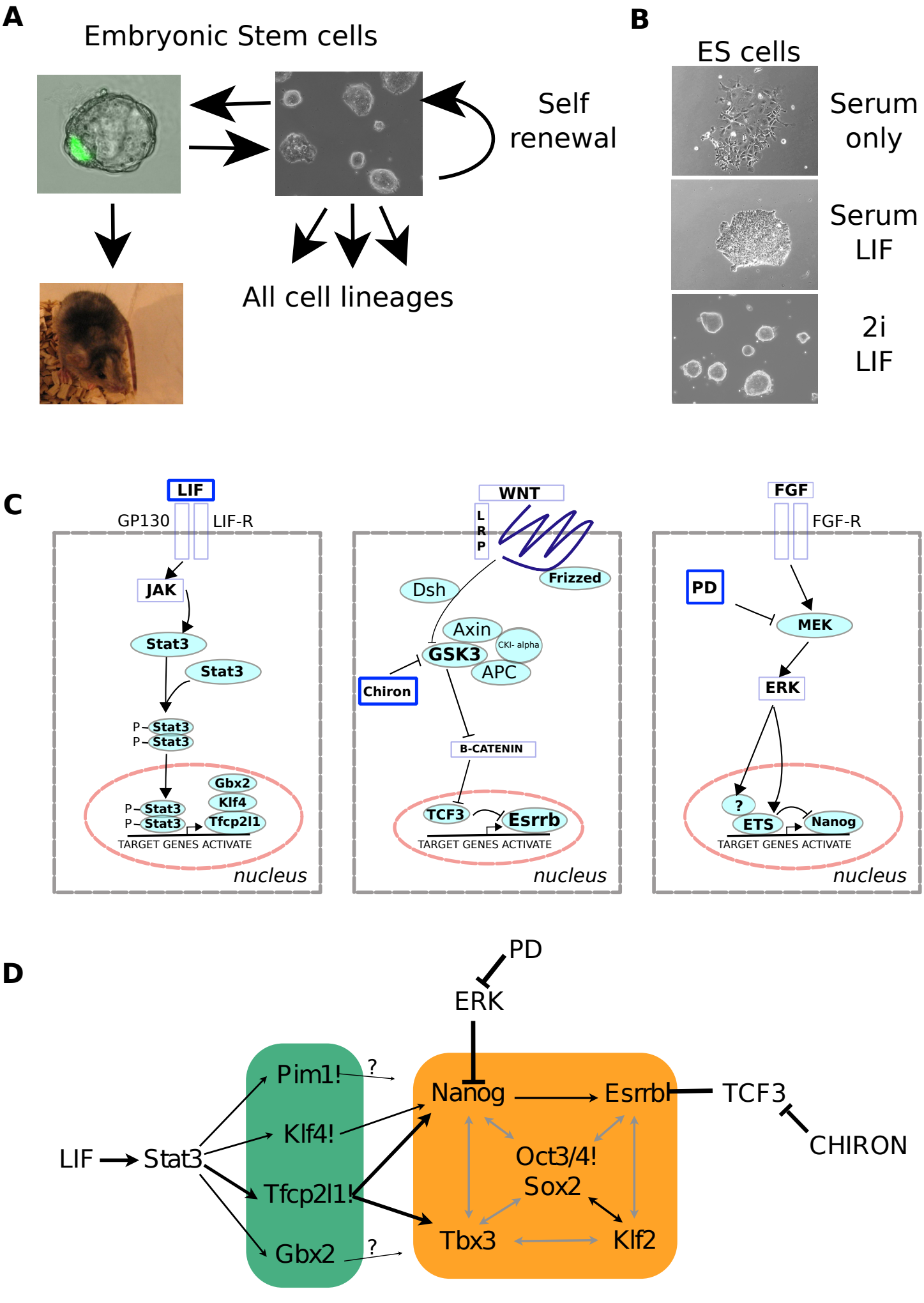

FIGURE 2

A) Overview of cellular metabolism. The major cellular metabolic pathways (indicated in red): Glycolysis, pentose phosphate pathway, β-oxidation, Krebs cycle and oxidative phosphorylation (OxPHOS). Each of these pathways produces metabolites that are required to fuel cell growth via the production of energy (ATP), nucleotides, lipids, amino acids and fatty acids (indicated in green). The most efficient pathway for the production of energy is OxPHOS, which produces significantly more ATP than Glycolysis. ADP, adenosine diphosphate; ATP, adenosine triphosphate; ATPase, ATP synthase; ETC, electron transport chain; F6P, fructose 6 phosphate; G6P, Glucose 6 phosphate; ROS, reactive oxygen species; TCA, tricarboxylic acid. (Image based on review Julie Mathieu and Hannele Ruohola-Baker 2017).

B) Representative scheme of mitochondrial DNA with the protein-encoding regions and tRNA-encoding genes.

(http://commons.wikimedia.org/wiki/Image:Mitochondrial_DNA_it.png)

C) An electron transport chain (ETC) in mammals consists in four enzyme complexes (complexes I-IV), and two intermediary substrates (coenzyme Q and cytochrome c). Complex I (NADH coenzyme Q reductase) accepts electrons from the Krebs cycle electron carrier nicotinamide adenine dinucleotide (NADH), and passes them to coenzyme Q (ubiquinone), which also receives electrons from complex II (succinate dehydrogenase). UQ passes electrons to complex III (cytochrome bc1 complex), which passes them to cytochrome c (cyt c). Cyt c passes electrons to Complex IV (cytochrome c oxidase), this complex carrier the proton out of the membrane and finally this gradient is used by the ATP synthase (complex V) to produce ATP, the only form of energy used by the cell. In orange is specified the subunits of respiratory chain codified only by the mitochondrial DNA. In red is reported the function of Rotenone and its target (complex I). (Image modified from Frontiers in Bioscience, January, 2009 -Mitochondria: from bioenergetics to the metabolic regulation of carcinogenesis Bellance Nadege1)

D) Graphic representation of different derived in vitro cells in the first stages of development. Naïve ESCs derive from the pre-implantation Blastocyst and shows a peculiar bivalent metabolism that equally use Glycolysis and OXPHOS, although mitochondria are immature with a spherical morphology and less dense cristae. Primed ESCs derive from post-implantation Blastocyst and their metabolism is exclusively glycolytic. Mitochondria in Primed ESCs show a mixture of immature and relative more mature morphology. Differentiated cells present full mature mitochondria and metabolism switch from glycolytic to OXPHOS but all the major metabolic pathways remain active. (Image based on review Julie Mathieu and Hannele Ruohola-Baker 2017).

FIGURE 2 intro

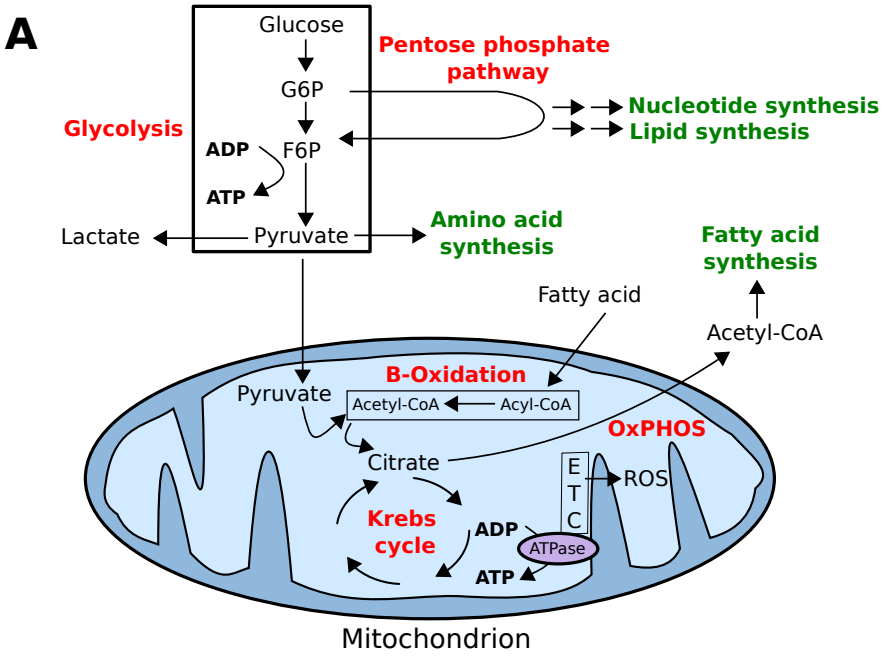

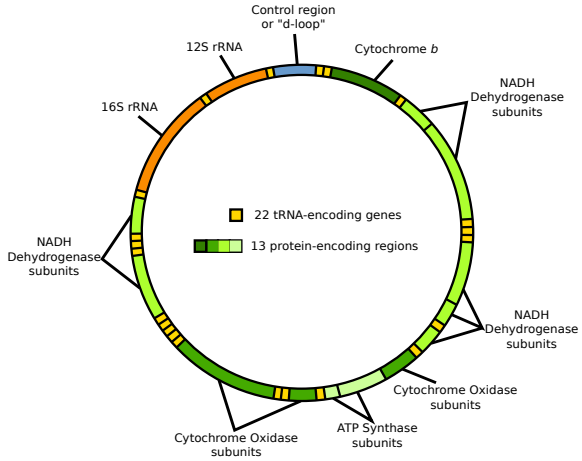

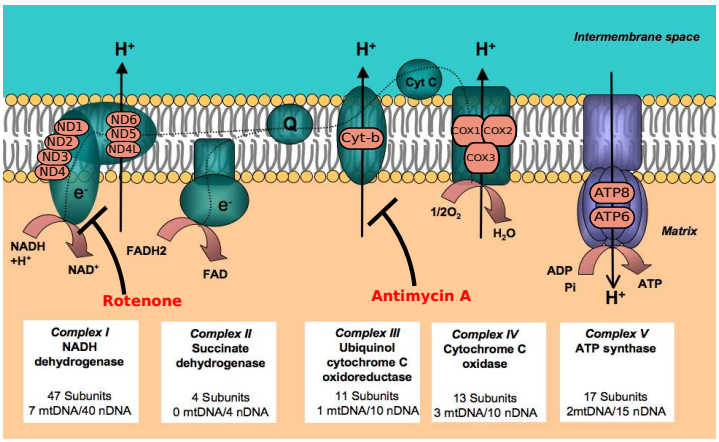

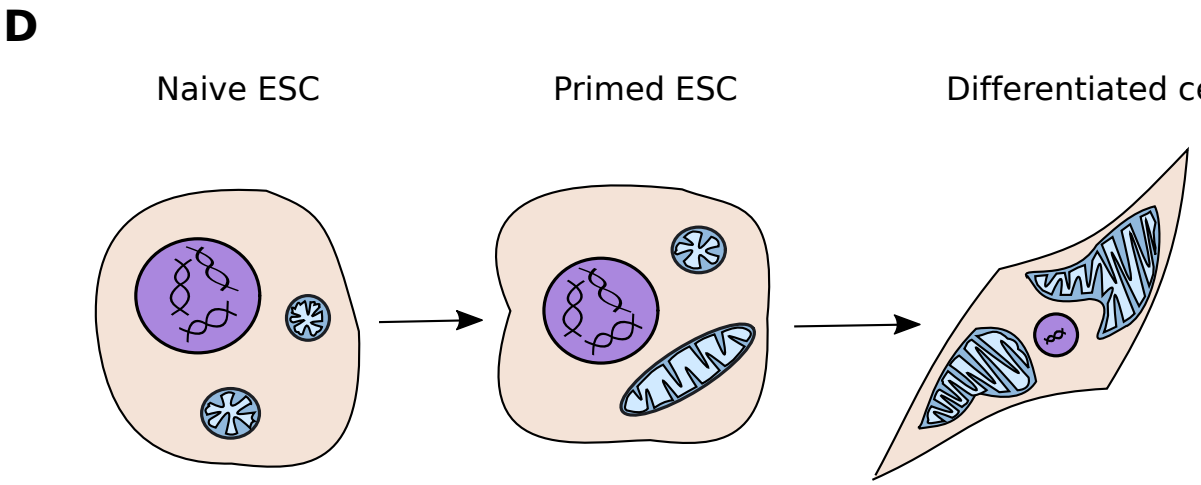

FIGURE 3

A) Proliferation assay of Stat3+/+ and Stat3-/- cells cultured in N2B27-based 2i media either in the presence or in the absence of LIF. Cells were seeded and scored for four consecutive days. Scores were normalized to day 1. Mean and s.d. of three technical replicates.

B) Trypan blue assay on Stat3+/+ cells cultured in 2i or 2i+LIF and Stat3-/- cells in 2i+LIF. Equal numbers of cells ware pleated and were cultured in 2i or 2i+LIF conditions. At regular intervals of 24h the cells were detached, treated with Trypan blue (a specific dye for dead cells) and counted. Histogram shows the percentage of viable cells in the three conditions. No significant difference in the percentage of viable cells is observed. Mean and s.e.m of two independent experiments is shown.

C) Scatter plot showing RNA-seq data from Stat3+/+ cells cultured in 2i and stimulated with LIF for 1 h (Martello et al, 2013). Absolute expression is shown in RPKM. Green dots indicate known LIF targets that serve as positive controls. Mitochondrial-encoded transcripts are represented as orange dots. Only genes with FC > 1.7 and a P-value < 0.05 are shown.

D) Heatmap showing mean normalized expression of 13 mitochondrial transcripts encoding 4 subunits of the mitochondrial respiratory chain. RNA-seq data are from Stat3+/+ and Stat3 -/- cells were expanded in 2i media without LIF and treated with LIF for 1 or 24 h.

E) Gene expression analysis by RT–qPCR of Stat3+/+ (blue) and Stat3 -/- (red) cells cultured in 2i and treated with LIF for 1 h, 4 h or 4 days. Data are normalized to unstimulated 2i cultures. Beta-actin served as an internal control. Mean and s.e.m. of three independent experiments. Unpaired t-test: *P < 0.05, **P < 0.01, ***P < 0.001.

FIGURE 3

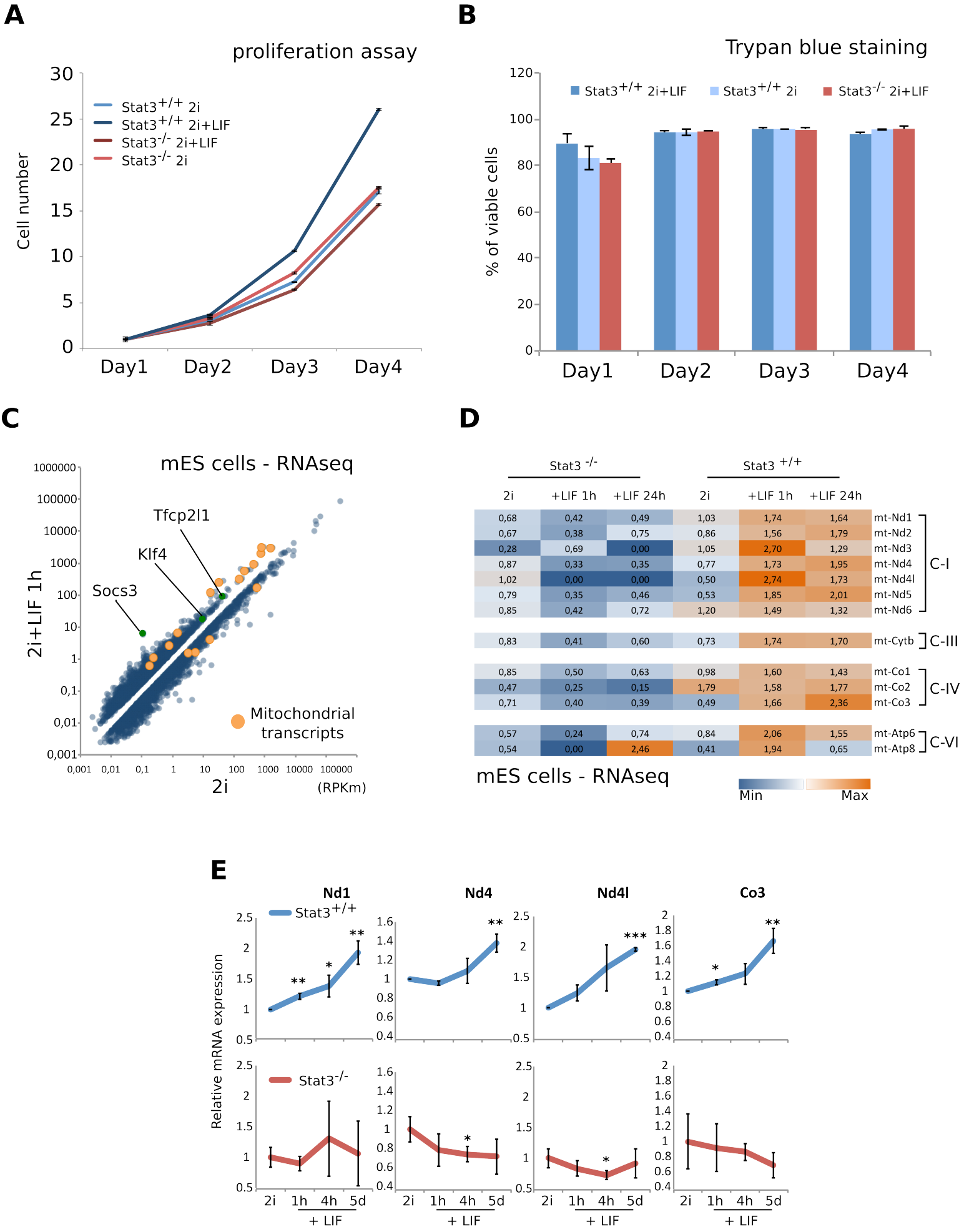
A
proliferation assay
Cell number
Stat3+/+ 2i
Stat3+/+ 2i+LIF
Stat3-/- 2i+LIF
Stat3-/- 2i
Day1
Day2
Day3
Day4
B
Trypan blue staining
% of viable cells
Stat3+/+ 2i+LIF
Stat3+/+ 2i
Stat3-/- 2i+LIF
C
mES cells - RNAseq
2i+LIF 1h
2i
(RPKm)
Tfcp2l1
Klf4
Socs3
Mitochondrial transcripts
D
Stat3 -/-
Stat3 +/+
2i
+LIF 1h
+LIF 24h
mt-Nd1 0,68 0,42 0,49 1,03 1,74 1,64
mt-Nd2 0,67 0,38 0,75 0,86 1,56 1,79
mt-Nd3 0,28 0,69 0,00 1,05 2,70 1,29
mt-Nd4 0,87 0,33 0,35 0,77 1,73 1,95
mt-Nd4l 1,02 0,00 0,00 0,50 2,74 1,73
mt-Nd5 0,79 0,35 0,46 0,53 1,85 2,01
mt-Nd6 0,85 0,42 0,72 1,20 1,49 1,32
C-I
mt-Cytb 0,83 0,41 0,60 0,73 1,74 1,70
C-III
mt-Co1 0,85 0,50 0,63 0,98 1,60 1,43
mt-Co2 0,47 0,25 0,15 1,79 1,58 1,77
mt-Co3 0,71 0,40 0,39 0,49 1,66 2,36
C-IV
mt-Atp6 0,57 0,24 0,74 0,84 2,06 1,55
mt-Atp8 0,54 0,00 2,46 0,41 1,94 0,65
C-VI
mES cells - RNAseq
Min
Max
E
Nd1
Nd4
Nd4l
Co3
Stat3+/+
Stat3-/-
Relative mRNA expression
2i
1h
4h
5d
+ LIF

FIGURE 4

A) Schematic representation of D-loop-Lux reporter construct used for luciferase assays.

B) Luciferase assay on ES cells transfected with D-loop-Lux reporter plasmid and Stat3 in the presence or in the absence of LIF for 48 h; p53 was previously shown to activate a similar reporter construct (Heyne et al, 2004) and therefore was used as a positive control. Increased expression of Stat3 enhances luciferase activity. Mean and s.e.m. of four independent experiments. Unpaired t-test: *P < 0.05.

C) Diagram highlighting available ChIP-seq results (GSM288353) of Stat3 binding on the D-loop. A, B, and C indicate regions where primers for ChIP-PCR analysis were designed.

D) Chromatin immunoprecipitation (ChIP) was performed using anti-Stat3 or a rabbit control IgG antibody in Rex1-GFP cells (Wray et al, 2010) cultured in LIF and serum conditions in the presence of blasticidin to reduce heterogeneity of the culture. ChIP-PCR was performed with primers located on three regions of the D-loop (A, B, C), as indicated in (D). Mean and s.d. of two independent experiments are shown.

E) Representative confocal images of Stat3+/+ cells subjected to proximity ligation assay (PLA) by using anti-Stat3 and anti-Atad3 antibodies. Only when the two proteins are close to each other, an enzymatic reaction takes place, producing discrete fluorescent red dots in the nanometer range (bottom). Anti-Stat3 or anti-Atad3 alone was used to assess the assay specificity (top and center, respectively). DAPI serves as a nuclear counterstain. Scale bar, 10 lm. The histogram shows the quantification of PLA performed on Stat3+/+ cells. The number of red dots/cell is plotted. Note that when cells are stained with both antibodies, the number of dots increases significantly, suggesting close proximity between Stat3 and the nucleoids marker Atad3 (light orange bar). Mean and s.e.m. of > 15 cells for each sample are shown. Unpaired t-test: *P < 0.05.

FIGURE 4

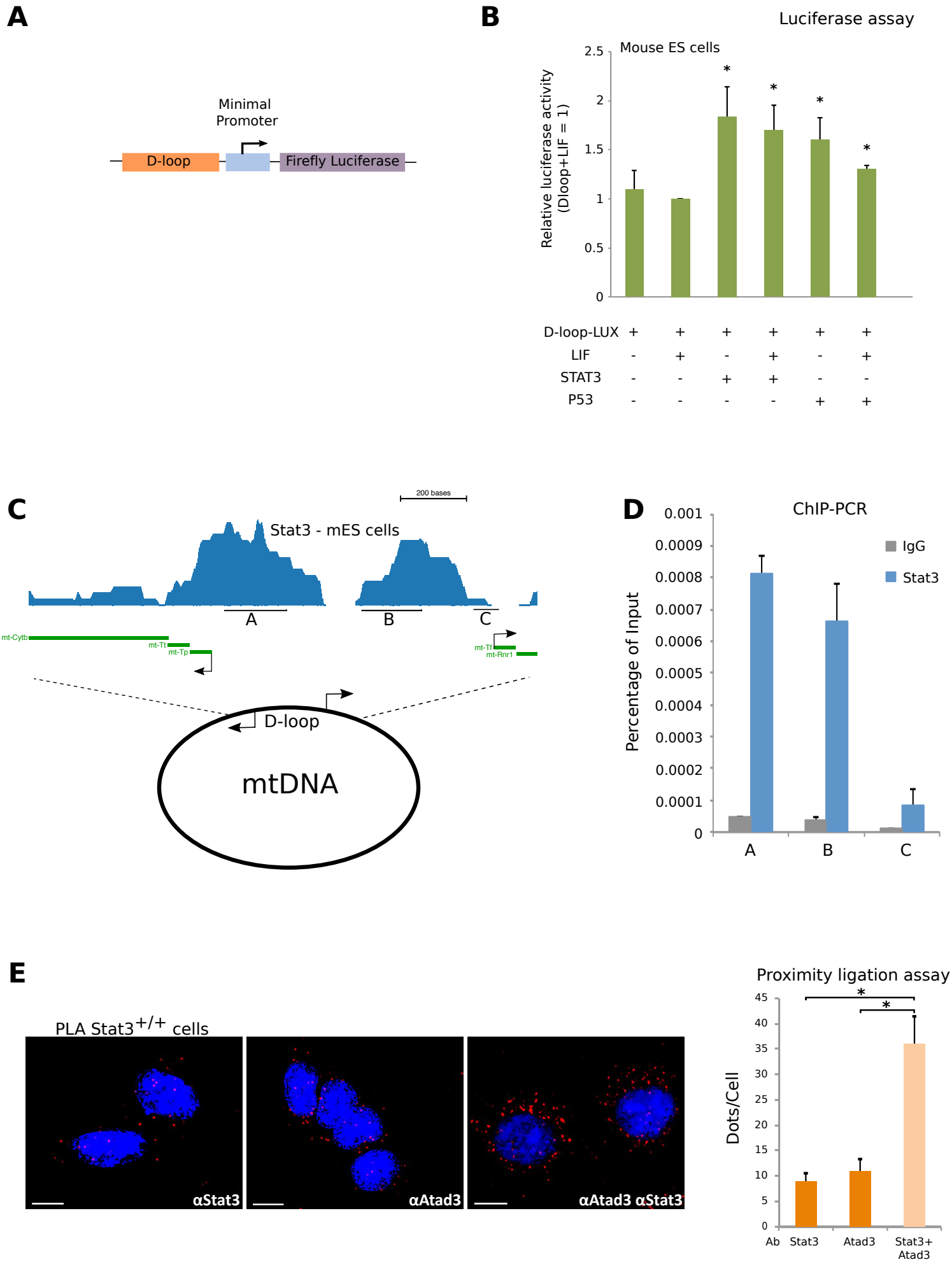
A
Minimal
Promoter
D-loop
Firefly Luciferase
B
Luciferase assay
Mouse ES cells
Relative luciferase activity
(Dloop+LIF = 1)
2.5
2
1.5
1
0.5
0
*
*
*
*
D-loop-LUX + + + + + +
LIF - + - + - +
STAT3 - - + + - -
P53 - - - - + +
C
200 bases
Stat3 - mES cells
A
B
C
mt-Cytb
mt-Tt
mt-Tp
mt-Tf
mt-Rnr1
D-loop
mtDNA
D
ChIP-PCR
IgG
Stat3
Percentage of Input
0.001
0.0009
0.0008
0.0007
0.0006
0.0005
0.0004
0.0003
0.0002
0.0001
0
A
B
C
E
PLA Stat3+/+ cells
αStat3
αAtad3
αAtad3 αStat3
Proximity ligation assay
Dots/Cell
45
40
35
30
25
20
15
10
5
0
*
*
Ab
Stat3
Atad3
Stat3+
Atad3

FIGURE 5

A) Oxygen consumption rate (OCR) measured by Seahorse extracellular flux assay of Stat3+/+ and Stat3-/- cells maintained in 2i condition in the presence of LIF; 200 nM FCCP (a mitochondria uncoupler) treatment resulted in higher OCR increase in Stat3+/+ compared to Stat3-/- cells, showing a higher level of maximal mitochondrial electron transport chain (ETC) activity in Stat3+/+ cells. Injection of 200 nM antimycin shows similar non-mitochondrial respiration rates for both Stat3+/+ and Stat3-/- cells. Mean and s.e.m. of 5 technical replicates are shown.

B) Oxygen consumption rate (OCR) of Stat3+/+ cells cultured in 2i conditions without LIF or with LIF for several passages; 200 nM FCCP and 200 nM antimycin were injected and resulted in a higher mitochondrial respiration activity in cells cultured in the presence of LIF. Mean and s.e.m. of 4 replicates are shown.

C) Relative changes in oxygen consumption after 200 nM FCCP treatment of Stat3+/+ cells cultured in 2i media in the presence (dark blue bars) and absence of LIF (light blue bars). Mean and s.e.m. of > 4 technical replicates of three independent experiments are shown. Unpaired t-test: *P < 0.05.

D) Western blot of Stat3+/+ cells cultured in the presence or absence of LIF. Note that protein levels of two mitochondrial markers (TOM20 and TIMM23) do not change in the absence of LIF. GAPDH was used as a loading control. Relative mean intensity is shown below each band**.**

E) Mitochondrial DNA expression analysis of Stat3+/+ cells maintained in 2i in the presence (dark blue bars) or absence (light blue bars) of LIF. The abundance of 3 mitochondrial genomic loci was measured and normalized to a nuclear genomic locus on chromosome 3. Mean and s.e.m. of three independent biological replicates are shown.

FIGURE 5

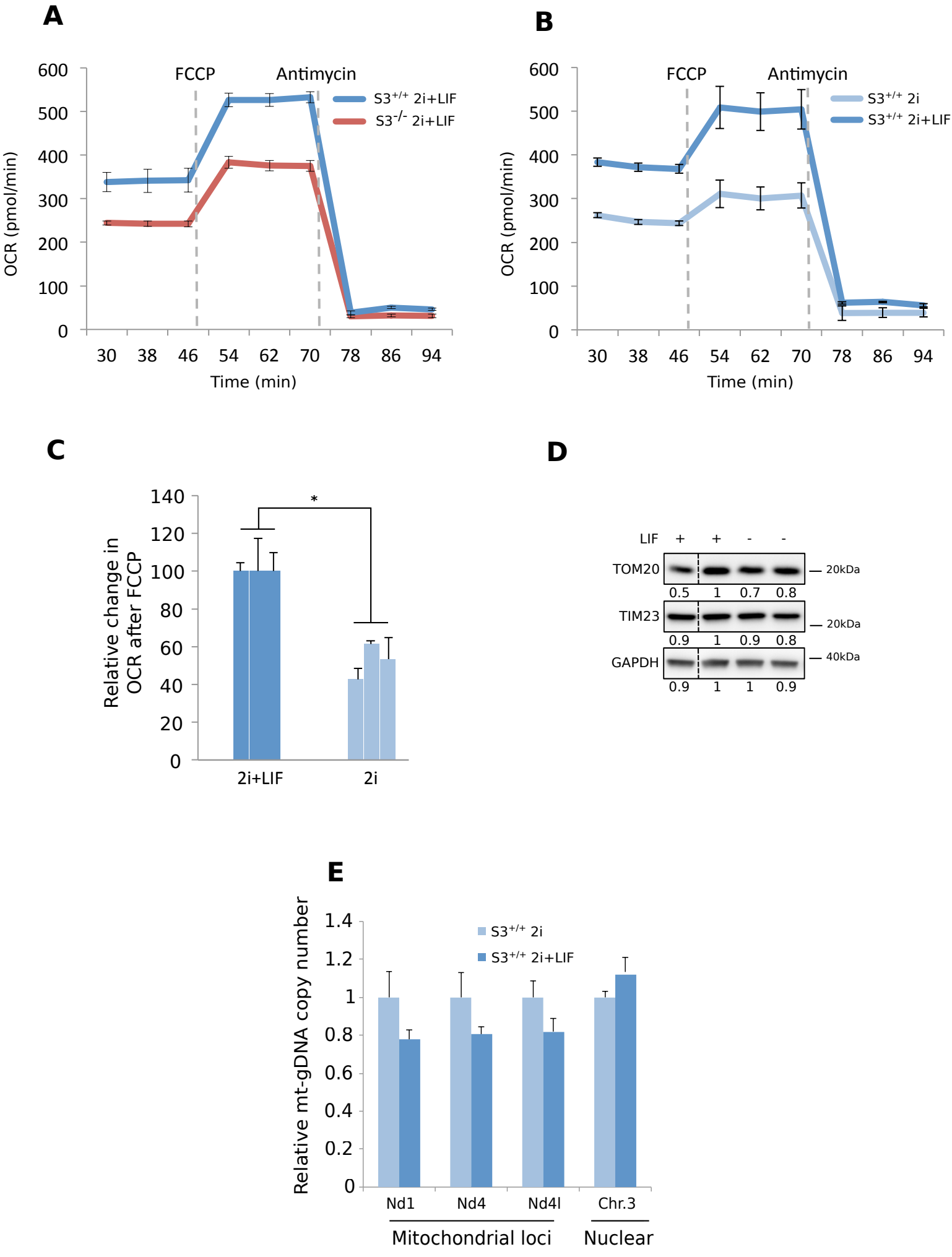
A
B
FCCP
Antimycin
OCR (pmol/min)
Time (min)
S3+/+ 2i+LIF
S3-/- 2i+LIF
S3+/+ 2i
C
Relative change in OCR after FCCP
2i+LIF
2i
*
D
LIF + + - -
TOM20
TIM23
GAPDH
20kDa
40kDa
0.5 1 0.7 0.8
0.9 1 0.9 0.8
0.9 1 1 0.9
E
Relative mt-gDNA copy number
Nd1
Nd4
Nd4l
Chr.3
Mitochondrial loci
Nuclear

FIGURE 6

A) Relative changes in oxygen consumption of Stat3+/+ cells after treatment with increasing doses of Rotenone. Basal levels of OCR were measured before Rotenone treatment and used to calculate the relative change in OCR. Note that 50nM Rotenone is sufficient to reduce mitochondrial respiration of 70%. Mean and s.e.m. of 5 biological replicates is shown.

B) Flow cytometry analysis after double staining with annexin V and propidium iodide in ES cells. The combination of annexin V-FITC and propidium iodide allows the distinction between viable cells (unstained) bottom left quadrants, early apoptotic cells (annexin V-FITC positive) bottom right quadrants, late apoptotic and/or necrotic cells (annexin V-FITC and propidium iodide positive) top right quadrants. ES cells were treated with increasing concentrations of rotenone from 50 nM to 200 nM for 48 h. A slight increase in cell death could be observed only at a concentration of 200 nM of rotenone. In each quadrant, the mean and s.e.m. of three independent experiments are indicated.

C) Proliferation assay of Stat3+/+ and Stat3-/- cells cultured in 2i. Cells were seeded and treated for 48 h with LIF and rotenone (orange bars), a Complex I inhibitor, as indicated. Scores were normalized to Stat3+/+ cells treated with LIF and DMSO. Proliferation was enhanced by LIF treatment in Stat3+/+ cells and reduced by rotenone treatment. Stat3-/- cells are more sensitive to rotenone treatment. Mean and s.e.m. of at least 2 independent experiments are shown. Unpaired t-test: *P < 0.05, ***P < 0.001. n.s.: non-significant

D) Relative changes in oxygen consumption of Stat3+/+ cells after treatment with increasing doses of Antimycin. Basal levels of OCR were measured before Antimycin treatment and used to calculate the relative change in OCR. Mean and s.e.m. of 5 biological replicates is shown.

E) Flow cytometry analysis after double staining with Annexin-V and Propidium Iodide in Stat3+/+ cells. Viable unstained cells are indicated on bottom left quadrants, early apoptotic cells (Annexin V-FITC positive) on bottom right quadrants and late apoptotic and/or necrotic cells (Annexin V-FITC and Propidium Podide positive) on top right quadrants. Cells were treated with increasing concentrations of Antimycin from 50nM to 200nM for 48 hours. In each quadrant the mean and s.e.m. of 3 independent experiments is indicated.

F) Proliferation assay of Stat3+/+ and Stat3-/- cells cultured in the presence of LIF showing the reduction in proliferation after 48-h treatment with increasing concentrations of antimycin A (50, 100, or 200 nM). Scores were normalized to WT cells treated with a vehicle (EtOH). Mean and s.e.m. of two independent experiments are shown. Unpaired t-test: **P < 0.01.

G) Gene expression analysis of Stat3+/+ cells transfected with control shRNA (SCR, dark green), and two independent shRNAs for a Complex I subunit (Ndufs3) (SH1 and SH2). Note that shRNAs for Ndufs3 downregulate gene expression of about 70%. Mean and s.d. of two independent experiments are shown. Unpaired t-test: *P < 0.05, **P < 0.01.

H) Relative changes in oxygen consumption after 200 nM FCCP treatment of Stat3+/+ cells transfected with control shRNA (dark green) and two different shRNAs for Ndufs3. Note that downregulation of the Complex I subunit results in decreased respiration. Mean and s.e.m. of > 4 technical replicates are shown. Unpaired t-test: *P < 0.05, ***P < 0.001.

I) Proliferation assay of control shRNA cells (dark green) and cells with downregulation of Ndufs3. Note that downregulation of the Complex I subunit results in decreased proliferation. Mean and s.e.m. of three independent experiments are shown.

FIGURE 6

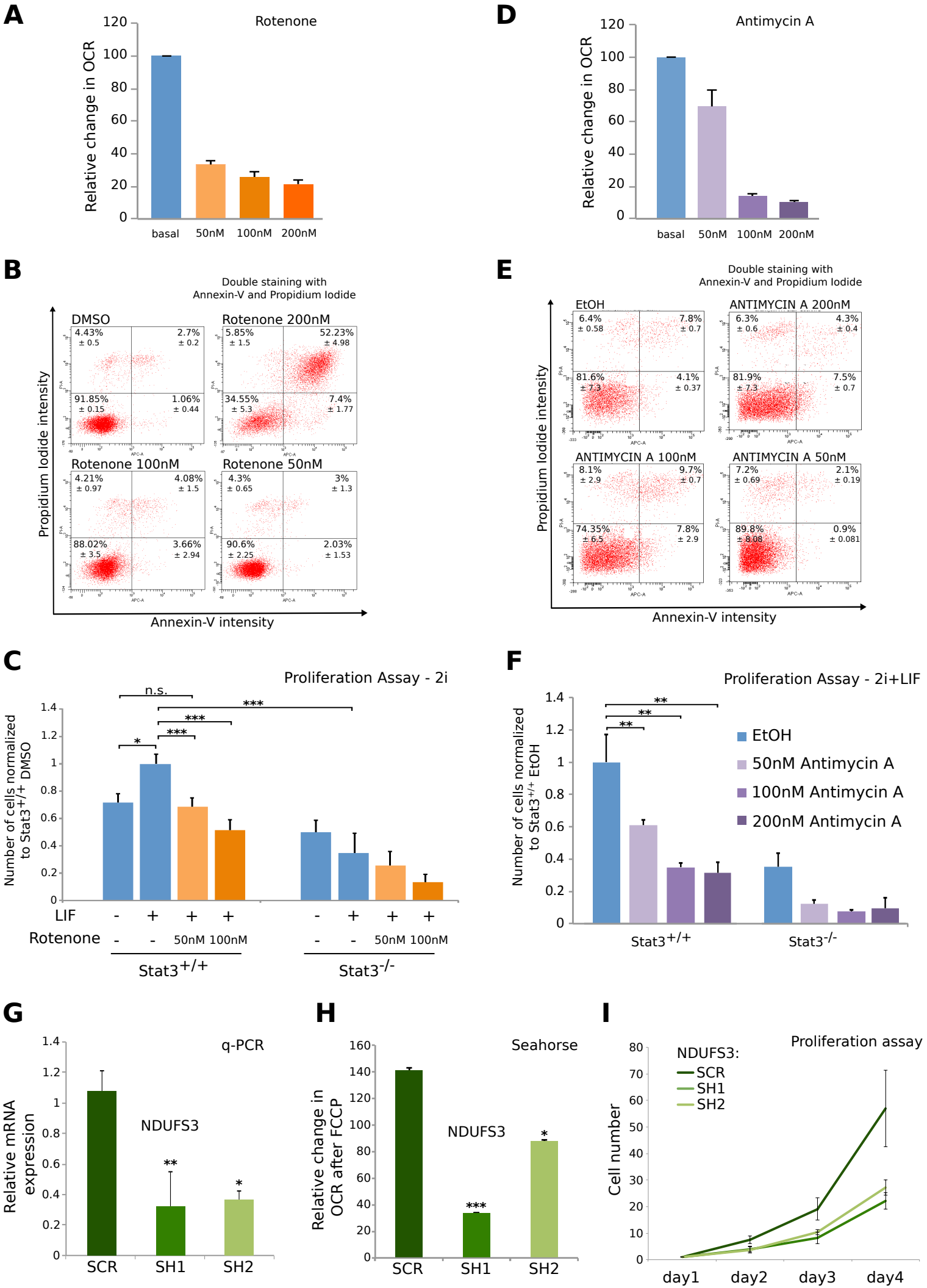
A
Rotenone
Relative change in OCR
120
100
80
60
40
20
0
basal
50nM
100nM
200nM
D
Antimycin A
Relative change in OCR
120
100
80
60
40
20
0
basal
50nM
100nM
200nM
B
Double staining with
Annexin-V and Propidium Iodide
DMSO
4.43% ± 0.5
2.7% ± 0.2
91.85% ± 0.15
1.06% ± 0.44
Rotenone 200nM
5.85% ± 1.5
52.23% ± 4.98
34.55% ± 5.3
7.4% ± 1.77
Rotenone 100nM
4.21% ± 0.97
4.08% ± 1.5
88.02% ± 3.5
3.66% ± 2.94
Rotenone 50nM
4.3% ± 0.65
3% ± 1.3
90.6% ± 2.25
2.03% ± 1.53
Propidium Iodide intensity
Annexin-V intensity
E
Double staining with
Annexin-V and Propidium Iodide
EtOH
6.4% ± 0.58
7.8% ± 0.7
81.6% ± 7.3
4.1% ± 0.37
ANTIMYCIN A 200nM
6.3% ± 0.6
4.3% ± 0.4
81.9% ± 7.3
7.5% ± 0.7
ANTIMYCIN A 100nM
8.1% ± 2.9
9.7% ± 0.7
74.35% ± 6.5
7.8% ± 2.9
ANTIMYCIN A 50nM
7.2% ± 0.69
2.1% ± 0.19
89.8% ± 8.08
0.9% ± 0.081
Propidium Iodide intensity
Annexin-V intensity
C
Proliferation Assay - 2i
Number of cells normalized to Stat3+/+ DMSO
1.4
1.2
1
0.8
0.6
0.4
0.2
0
n.s.
*
***
***
***
LIF - + + + - + + +
Rotenone - - 50nM 100nM - - 50nM 100nM
Stat3+/+
Stat3-/-
F
Proliferation Assay - 2i+LIF
Number of cells normalized to Stat3+/+ EtOH
1.4
1.2
1
0.8
0.6
0.4
0.2
0
**
**
**
EtOH
50nM Antimycin A
100nM Antimycin A
200nM Antimycin A
Stat3+/+
Stat3-/-
G
q-PCR
Relative mRNA expression
1.4
1.2
1
0.8
0.6
0.4
0.2
0
NDUFS3
**
*
SCR
SH1
SH2
H
Seahorse
Relative change in OCR after FCCP
160
140
120
100
80
60
40
20
0
NDUFS3
***
*
SCR
SH1
SH2
I
Proliferation assay
Cell number
80
70
60
50
40
30
20
10
0
NDUFS3:
SCR
SH1
SH2
day1
day2
day3
day4

FIGURE 7

A) Experimental approach used to characterize the functional role of Stat3 on cell proliferation and mitochondrial activity.

B) Western blot of Stat3+/+ cells cultured in the presence or absence of LIF, Stat3-/- cells cultured in 2i + LIF, and two clones of Stat3-/- cells transfected with a full-length form of Stat3 cultured in 2i + LIF. Relative mean intensity is shown below each band. Note that Stat3 protein levels in clone A and B are comparable to the endogenous levels of the control. GAPDH was used as a loading control.
C) Gene expression analysis of Stat3+/+ cells, Stat3-/- cells, and two Stat3 rescue clones (Stat3.A/B) cultured in the absence or presence of LIF. Note that both clones respond to LIF and activate Stat3 direct target Socs3.

D) Proliferation assay of Stat3+/+ cells, Stat3-/- cells, and Stat3.A/B rescue clones cultured in the presence of LIF. Cells were seeded and scored for 4 days. Scores were normalized to day 1. Mean and s.e.m. of two independent biological replicates of a representative experiment are shown.

E) Western blot of total and mitochondrial fractions of Stat3+/+, Stat3-/- cells, and two MLS-Stat3 clones cultured in 2i + LIF. The nuclear protein TRIM33 and mitochondrial marker TOM20 confirmed successful mitochondrial isolation. Note that MLS-Stat3 is enriched in the mitochondrial fraction, suggesting correct localization of the fusion protein.

F) Gene expression analysis of Stat3+/+, Stat3-/- cells, and three MLS-Stat3 clones cultured in the presence of LIF. MLS-Stat3 specifically induces expression of mitochondrial markers with negligible effects on the nuclear target Socs3. Mean and s.d. of two technical replicates.

G) Chromatin immunoprecipitation (ChIP) performed using anti-Stat3 or a rabbit control IgG antibody in Stat3 -/- and MLS-Stat3 cells cultured in 2i + LIF conditions. ChIP-PCR was performed with primers located on three regions of the D-loop (A, B, C). Note that 2 D-loop regions are significantly enriched in MLS-Stat3 compared to Stat3-/- cells. Mean and s.e.m. of three independent experiments are shown. Unpaired t-test: *P < 0.05, **P < 0.01.

H) Left: representative confocal images of Stat3-/- and MLS-Stat3 cells subjected to proximity ligation assay (PLA) by using anti-Stat3 and anti-Atad3 antibodies. DAPI serves as a nuclear counterstain. Red dots indicate spacial proximity between Stat3 and the nucleoids marker Atad3. Right: histogram showing quantification of PLA performed on Stat3+/+, Stat3-/-, and MLS-Stat3 cells. A number of red dots/cell are plotted. Note that double staining in MLS-Stat3 cells results in increased number or red dots compared to Stat3-/- cells. Mean and s.e.m. of > 15 cells for each sample are shown. Unpaired t-test: **P < 0.01, ***P < 0.001. Scale bar, 10 μm.

I) Left: Proliferation assay of Stat3+/+, Stat3-/- cells, and three MLS-Stat3 clones cultured in the presence of LIF. Cells were seeded and scored for 4 days. Mean and s.e.m. of two technical replicates of a representative experiment are shown.
I) Right: Representative bright field images of Stat3+/+, Stat3-/-, and one MLS-Stat3 clone cultured in 2i + LIF showing similar morphology, but note smaller colony size for Stat3-/- cells. Scale bar, 100 μm.

FIGURE 7

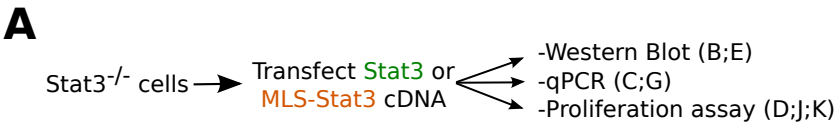
A
Stat3-/- cells
Transfect Stat3 or MLS-Stat3 cDNA
-Western Blot (B;E)
-qPCR (C;G)
-Proliferation assay (D;J;K)

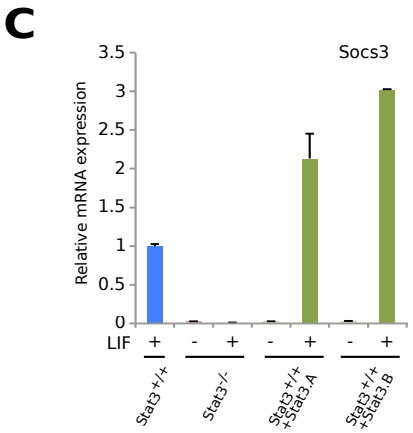
C
Socs3
Relative mRNA expression
LIF
Stat3+/+
Stat3-/-
Stat3+/+ +Stat3.A
Stat3+/+ +Stat3.B

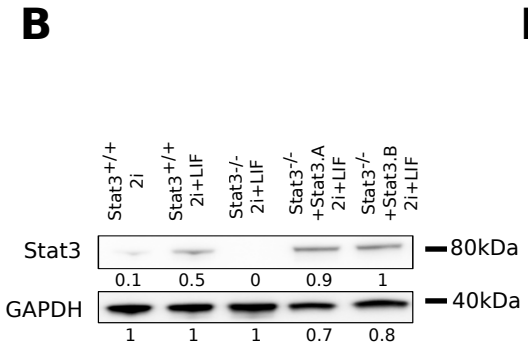
B
Stat3+/+ 2i
Stat3+/+ 2i+LIF
Stat3-/- 2i+LIF
Stat3-/- +Stat3.A 2i+LIF
Stat3-/- +Stat3.B 2i+LIF
Stat3
GAPDH
80kDa
40kDa

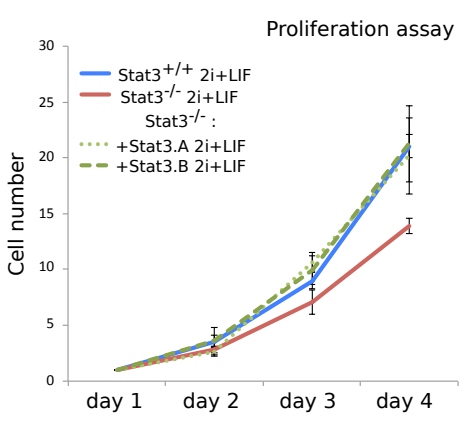
D
Proliferation assay
Stat3+/+ 2i+LIF
Stat3-/- 2i+LIF
Stat3-/- :
+Stat3.A 2i+LIF
+Stat3.B 2i+LIF
Cell number
day 1
day 2
day 3
day 4

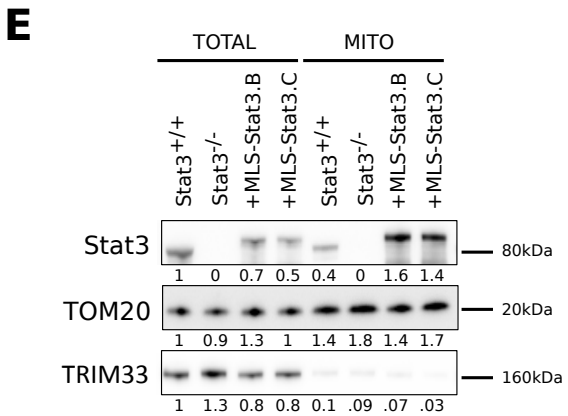
E
TOTAL
MITO
Stat3+/+
Stat3-/-
+MLS-Stat3.B
+MLS-Stat3.C
Stat3
TOM20
TRIM33
80kDa
20kDa
160kDa

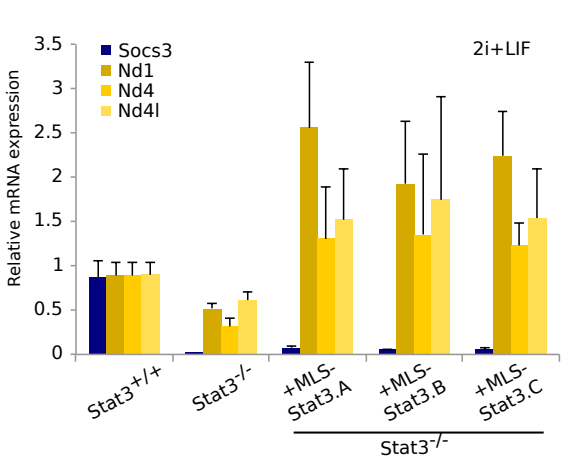
F
Socs3
Nd1
Nd4
Nd4l
2i+LIF
Relative mRNA expression
Stat3+/+
Stat3-/-
+MLS-Stat3.A
+MLS-Stat3.B
+MLS-Stat3.C
Stat3-/-

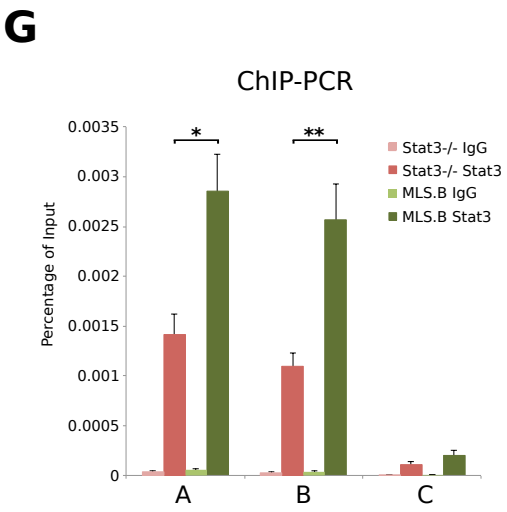
G
ChIP-PCR
Percentage of Input
Stat3-/- IgG
Stat3-/- Stat3
MLS.B IgG
MLS.B Stat3
A
B
C

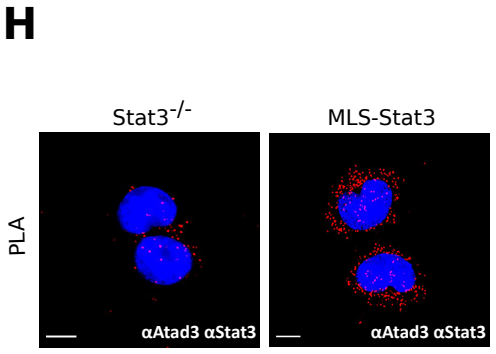
H
Stat3-/-
MLS-Stat3
PLA
αAtad3 αStat3
αAtad3 αStat3

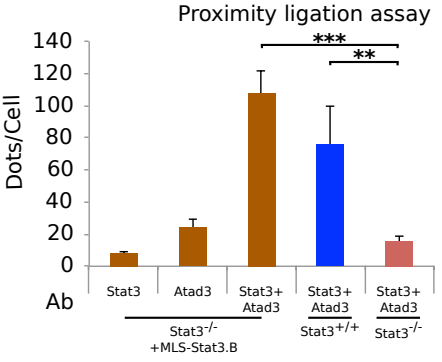
Proximity ligation assay
Dots/Cell
Ab
Stat3
Atad3
Stat3+ Atad3
Stat3-/- +MLS-Stat3.B
Stat3+/+
Stat3-/-

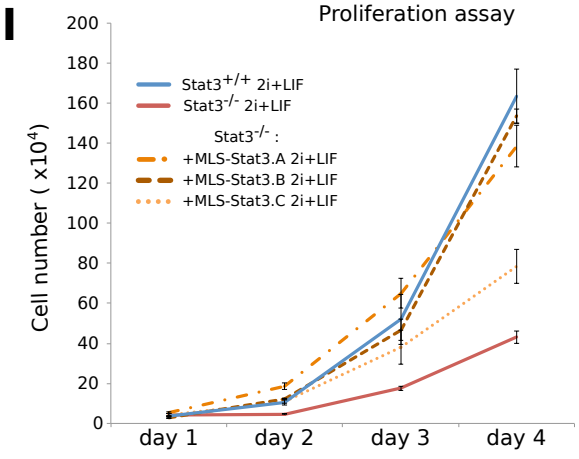
I
Proliferation assay
Cell number (x10^4)
Stat3+/+ 2i+LIF
Stat3-/- 2i+LIF
Stat3-/- :
+MLS-Stat3.A 2i+LIF
+MLS-Stat3.B 2i+LIF
+MLS-Stat3.C 2i+LIF
day 1
day 2
day 3
day 4

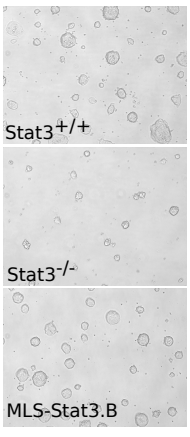
Stat3+/+
Stat3-/-
MLS-Stat3.B

FIGURE 8

A) Western blot for total STAT3 on Stat3+/+, -/- and MLS-S3-NES. Note the shift in molecular weight due to the presence of MLS and NES tag. Stat3 protein level in both MLS-S3-NES clones is lower than Stat3+/+ cells.

B) qPCR analysis of the Stat3 and its nuclear target gene Socs3. Gene expression analysis of Stat3+/+ cells, Stat3-/- cells, and two MLS-S3-NES clones (A/B) cultured in presence of LIF. Note that both clones have the same undetectable level of Socs3 as Stat3-/- cells.

C) Representative confocal images of Stat3+/+, -/- and MLS-S3-NES cells stained with anti-STAT3 and anti-ATAD3 antibodies. Merge image shows co-localization between STAT3 and the nucleoids marked by ATAD3; DAPI serves as a nuclear counterstain.

D) Proliferation assay of Stat3+/+, -/- cells, and two MLS-S3-NES clones cultured in the presence of LIF. Cells were seeded and scored for 4 consecutive days. Both clones present a partial rescue in the proliferative capacity.

E) Oxygen consumption rate (OCR) measured by Seahorse extracellular flux assay of Stat3+/+, -/- and MLS-S3-NES clones cells. MLS-S3-NES clones show a full rescue in the respiration capacity; both at the basal level and post FCCP treatment.

FIGURE 8

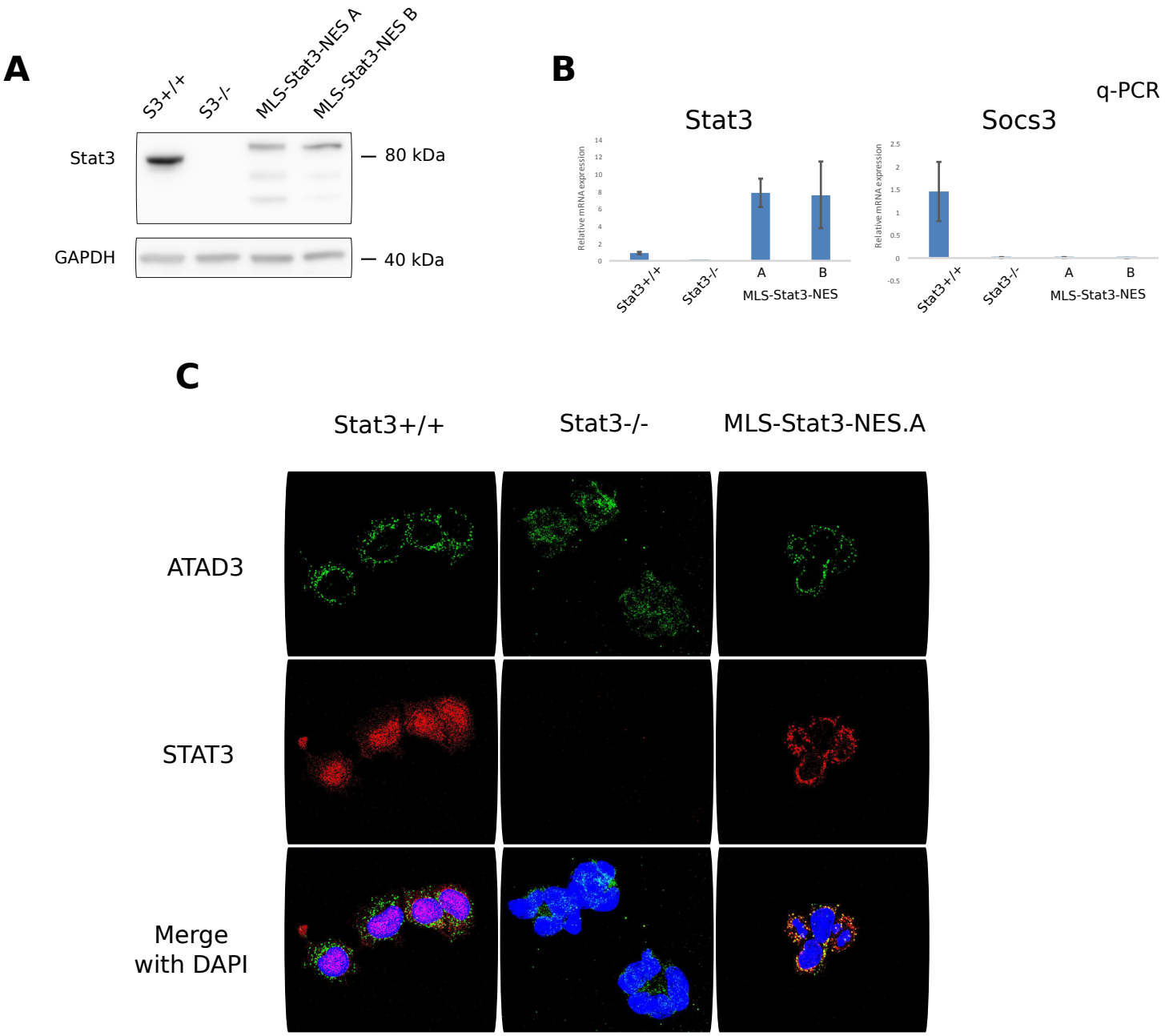
A
S3+/+
S3-/-
MLS-Stat3-NES A
MLS-Stat3-NES B
Stat3
80 kDa
GAPDH
40 kDa
B
q-PCR
Stat3
Socs3
Relative mRNA expression
Stat3+/+
Stat3-/-
A
B
MLS-Stat3-NES
C
Stat3+/+
Stat3-/-
MLS-Stat3-NES.A
ATAD3
STAT3
Merge
with DAPI
D
Proliferation assay
Cell number
Stat3+/+
Stat3-/-
MLS-Stat3-NES A
MLS-Stat3-NES B
day1
day2
day3
day4
E
Sea Horse
FCCP
Antimycin/Rotenone
OCR (pmoll/min)
Basal
Maximal
Time (min)

FIGURE 9

A) Principal component analysis of Metabolome in the Stat3+/+, -/- and MLS-S3-NES. This graphic representation shows that Stat3+/+ and -/- are clearly separated and MLS-S3-NES clones lie in between. Unit variance scaling is applied to rows; SVD with imputation is used to calculate principal components. X and Y axis show principal component 1 and principal component 2 that explain 32.4% and 23.1% of the total variance, respectively. Prediction ellipses are such that with probability 0.95, a new observation from the same group will fall inside the ellipse. N = 24 data points.

B) Heatmap of the metabolic analysis of Stat3+/+, -/- and MLS-S3-NES cells. Unsupervised hierarchical clustering correctly identifies 3 groups of cells. Rows are centered; unit variance scaling is applied to rows. Both rows and columns are clustered using correlation distance and average linkage. 27 rows, 24 columns.

C) Volcano plot shows the metabolites that are significantly more abundant in Stat3+/+ (blue dot) and Stat3-/- cells (red dot). Most of medium chain (partially oxidized) carnitine are high in Stat3-/- cells, which indicates that the Fatty Acid-Oxidation is impaired (red circle). Conversely, Stat3+/+ cells show a more abundant Krebs cycle's metabolite (blue circle). Notably, ATP is more abundant in Stat3-/- cells (yellow circle).

D) Graphic representation of the Krebs Cycle and quantification of individual metabolite abundance. Note that Stat3-/- cells have a reduced level in most of metabolites of TCA and in some cases MLS-S3- NES shows a rescue.

E) Heat map shows expression levels of Glycolysis genes in Stat3+/+, -/- and MLS-S3-NES cells. Unsupervised hierarchical clustering correctly identifies 3 groups of cells. Stat3-/- cells show increased expression of Glycolysis genes compared to the other cell lines.

F) Proliferation assay of Stat3+/+, -/- and MLS-S3-NES cells cultured in 2i plus LIF. Cells were seeded and treated for 72 h with different doses of 2-Deoxy-D-Glucose (2-DG), a Glucose competitor. Scores were normalized to untreated cells. Proliferation was more reduced by 2-DG treatment in Stat3-/- cells indicating that they have a higher dependency by Glucose.

FIGURE 9

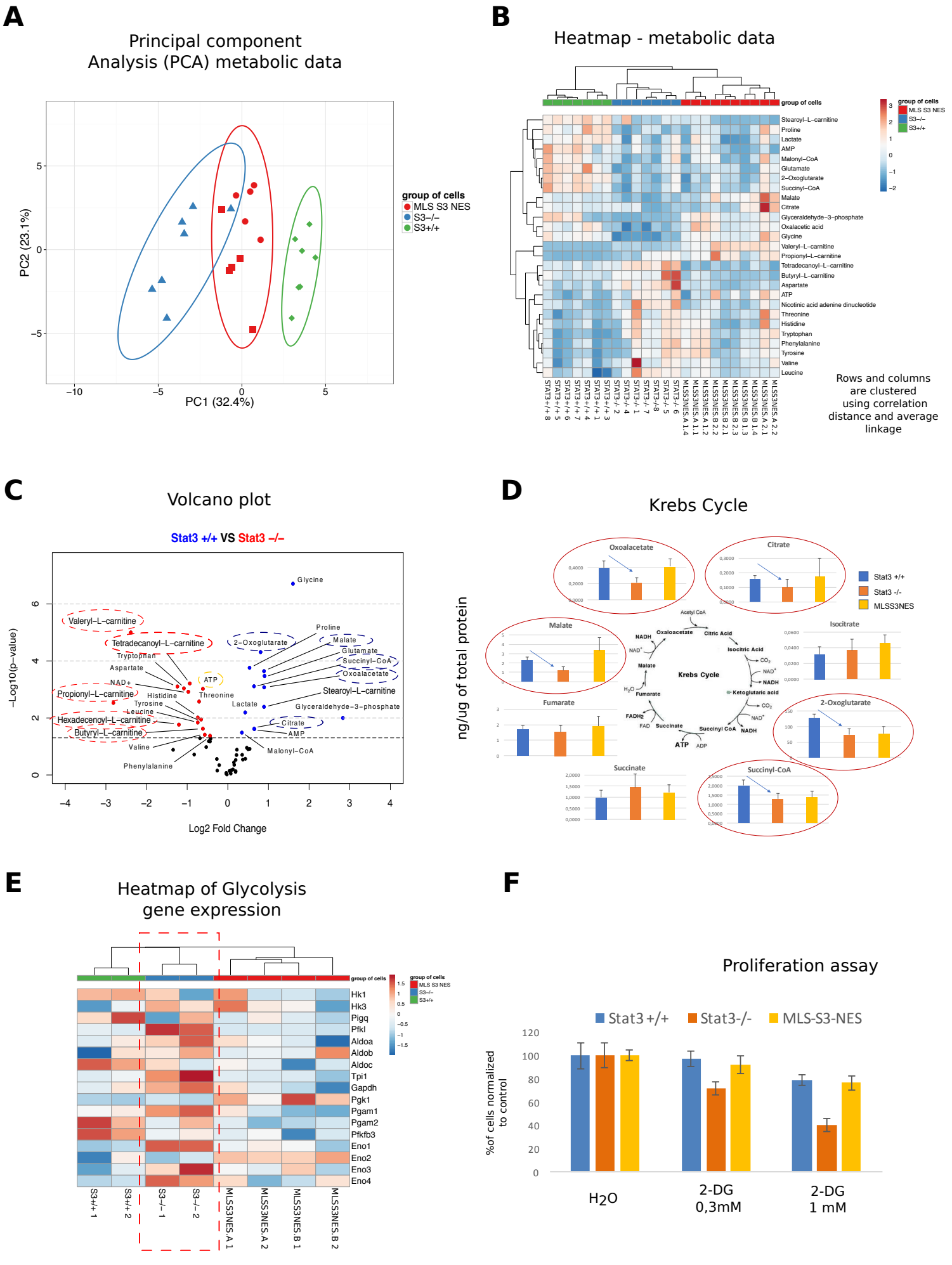
A
Principal component Analysis (PCA) metabolic data
PC2 (23.1%)
PC1 (32.4%)
group of cells
MLS S3 NES
S3−/−
S3+/+
B
Heatmap - metabolic data
group of cells
Stearoyl−L−carnitine
Proline
Lactate
AMP
Malonyl−CoA
Glutamate
2−Oxoglutarate
Succinyl−CoA
Malate
Citrate
Glyceraldehyde−3−phosphate
Oxalacetic acid
Glycine
Valeryl−L−carnitine
Propionyl−L−carnitine
Tetradecanoyl−L−carnitine
Butyryl−L−carnitine
Aspartate
ATP
Nicotinic acid adenine dinucleotide
Threonine
Histidine
Tryptophan
Phenylalanine
Tyrosine
Valine
Leucine
Rows and columns are clustered using correlation distance and average linkage
C
Volcano plot
Stat3 +/+ VS Stat3 −/−
−Log10(p−value)
Log2 Fold Change
Glycine
Valeryl−L−carnitine
Tetradecanoyl−L−carnitine
Tryptophan
Aspartate
NAD+
Propionyl−L−carnitine
Histidine
Tyrosine
Leucine
Hexadecenoyl−L−carnitine
Butyryl−L−carnitine
Valine
Phenylalanine
ATP
Threonine
Lactate
2−Oxoglutarate
Proline
Malate
Glutamate
Succinyl−CoA
Oxoalacetate
Stearoyl−L−carnitine
Glyceraldehyde−3−phosphate
Citrate
AMP
Malonyl−CoA
D
Krebs Cycle
ng/ug of total protein
Stat3 +/+
Stat3 -/-
MLSS3NES
Oxoalacetate
Citrate
Malate
Isocitrate
Fumarate
2-Oxoglutarate
Succinate
Succinyl-CoA
Acetyl CoA
Citric Acid
Isocitric Acid
Krebs Cycle
Ketoglutaric acid
Succinyl CoA
Succinate
Fumarate
Malate
Oxaloacetate
NADH
FADH2
FAD
ATP
ADP
E
Heatmap of Glycolysis gene expression
group of cells
MLS S3 NES
S3−/−
S3+/+
Hk1
Hk3
Pigq
Pfkl
Aldoa
Aldob
Aldoc
Tpi1
Gapdh
Pgk1
Pgam1
Pgam2
Pfkfb3
Eno1
Eno2
Eno3
Eno4
S3+/+ 1
S3+/+ 2
S3−/− 1
S3−/− 2
MLS3NES.A 1
MLS3NES.A 2
MLS3NES.B 1
MLS3NES.B 2
F
Proliferation assay
Stat3 +/+
Stat3-/-
MLS-S3-NES
%of cells normalized to control
H2O
2-DG 0,3mM
2-DG 1 mM

FIGURE 10

A) Oxygen consumption rate (OCR) measured by Seahorse extracellular flux assay of Stat3+/+, cultured with 2i LIF or without for 24 and 48 hours. Stat3+/+ cultured without 2iLIF decreased the respiration capacity in comparison to Stat3+/+ maintained in 2iLIF.

B) Representative bright field images of Stat3+/+, Stat3-/-, and two MLS-Stat3-NES clones cultured with or without 2i LIF for 24 hours. Images showing that morphology of Stat3-/- cells change more rapidly than Stat3+/+ cells and MLS-Stat3-NES clones during differentiation (black arrow indicate the cytoplasmic protrusion in Stat3-/- cells after 24h in a differentiation media).

C) Left: Alkaline phosphatase assay in Stat3+/+, -/- and MLS-S3-NES clones cultured with 2iLIF or without 2iLIF for 24h, 48h or 72h. Note that Stat3-/- cells escape more quickly from Pluripotent state and MLS-Stat3-NES rescues such effect.
C) Right: Alkaline phosphatase quantification with ImageJ tool.

D) Gene expression analysis by RT–qPCR of Stat3+/+ (blue), Stat3-/- (Orange) and two MLS-S3-NES (yellow & grey) clones cultured with 2iLIF or without 2iLIF for 24h or 48h. Early differentiation markers are more readily induced in Stat3-/- and MLS-Stat3 rescues this effect. Data are normalized to Stat3+/+ cells -48h 2iLIF. Beta-actin served as an internal control.

E) Model depicting the dual role of Stat3 as an inducer of nuclear transcription factors critical for maintenance and induction of naïve Pluripotency and, at the same time, as an activator of mitochondrial transcription and activity responsible for the high levels of respiration observed in naïve Pluripotent cells.

F) Model depicting the principal difference between ES and differentiated cells. Note that Stat3-/- cells are situated in a sort of formative state between the two state.

FIGURE 10

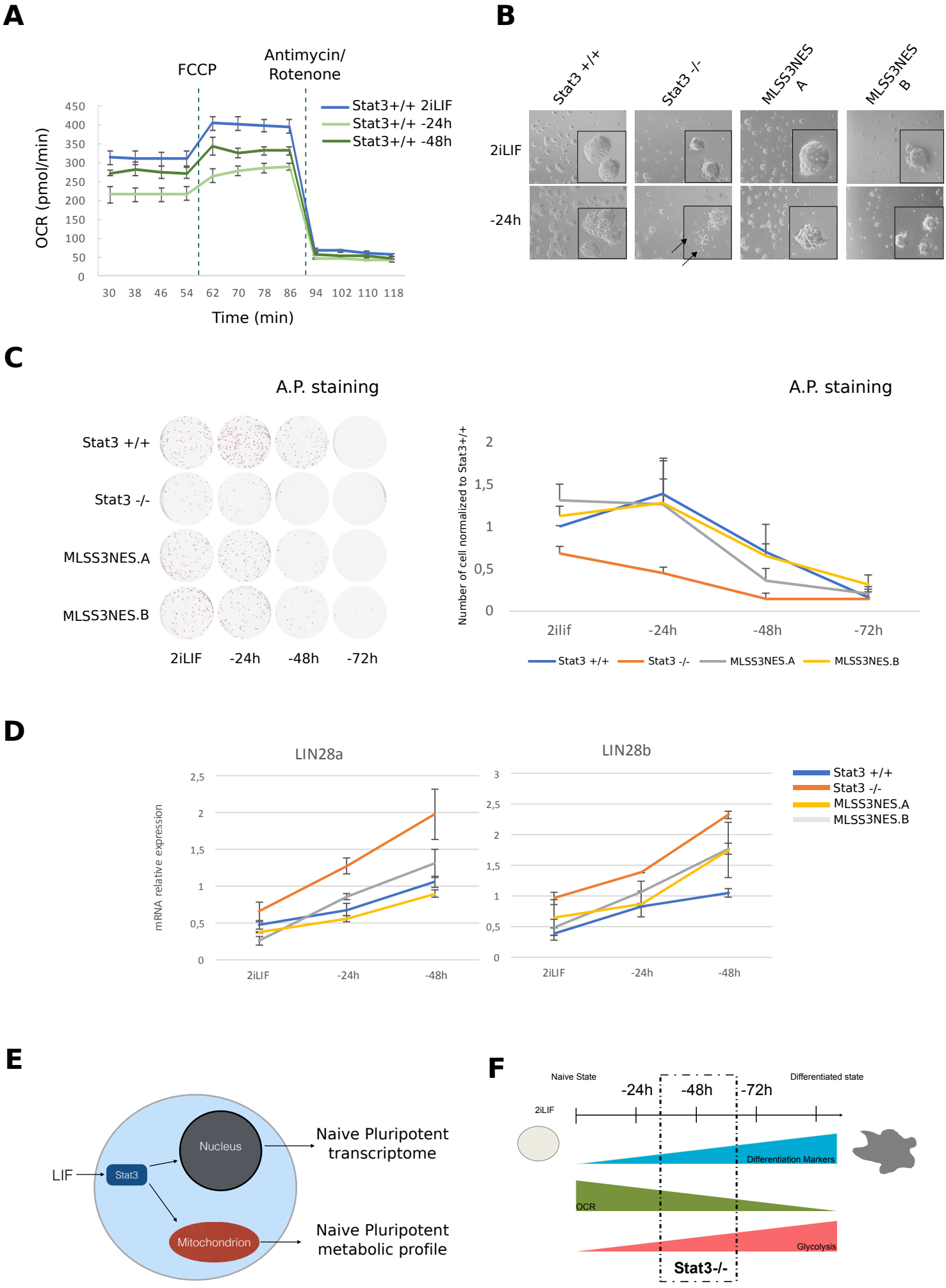
A
FCCP
Antimycin/
Rotenone
Stat3+/+ 2iLIF
Stat3+/+ -24h
Stat3+/+ -48h
OCR (pmol/min)
Time (min)
B
Stat3 +/+
Stat3 -/-
MLSS3NES A
MLSS3NES B
2iLIF
-24h
C
A.P. staining
Stat3 +/+
Stat3 -/-
MLSS3NES.A
MLSS3NES.B
2iLIF
-24h
-48h
-72h
A.P. staining
Number of cell normalized to Stat3+/+
D
LIN28a
LIN28b
mRNA relative expression
E
LIF
Stat3
Nucleus
Mitochondrion
Naive Pluripotent transcriptome
Naive Pluripotent metabolic profile
F
Naive State
Differentiated state
Differentiation Markers
OCR
Glycolysis
Stat3-/-

REFERENCES:

Berge, ten, D., Kurek, D., Blauwkamp, T., Koole, W., Maas, A., Eroglu, E., Siu, R.K., and Nusse, R. (2011). Embryonic stem cells require Wnt proteins to prevent differentiation to epiblast stem cells. Nat. Cell Biol. *13*, 1070–1075.

Carbognin, E., Betto, R.M., Soriano, M.E., Smith, A.G., and Martello, G. (2016). Stat3 promotes mitochondrial transcription and oxidative respiration during maintenance and induction of naive pluripotency. Embo J. *35*, 618–634.

Carey, B.W., Finley, L.W.S., Cross, J.R., Allis, C.D., and Thompson, C.B. (2015). Intracellular α-ketoglutarate maintains the pluripotency of embryonic stem cells. Nature *518*, 413–416.

Chen, X., Xu, H., Yuan, P., Fang, F., Huss, M., Vega, V.B., Wong, E., Orlov, Y.L., Zhang, W., Jiang, J., et al. (2008). Integration of external signaling pathways with the core transcriptional network in embryonic stem cells. Cell *133*, 1106–1117.

Doble, B.W., and Woodgett, J.R. (2003). GSK-3: tricks of the trade for a multi-tasking kinase. J. Cell. Sci. *116*, 1175–1186.

Duchen, M.R. (2004). Roles of mitochondria in health and disease. Diabetes *53 Suppl 1*, S96–S102.

Enzo, E., Santinon, G., Pocaterra, A., Aragona, M., Bresolin, S., Forcato, M., Grifoni, D., Pession, A., Zanconato, F., Guzzo, G., et al. (2015). Aerobic glycolysis tunes YAP/TAZ transcriptional activity. Embo J. *34*, 1349–1370.

Frezza, C., Cipolat, S., and Scorrano, L. (2007). Measuring mitochondrial shape changes and their consequences on mitochondrial involvement during apoptosis. Methods Mol. Biol. *372*, 405–420.

Garama, D.J., White, C.L., Balic, J.J., and Gough, D.J. (2016). Mitochondrial STAT3: Powering up a potent factor. Cytokine *87*, 20–25.

Gough, D.J., Corlett, A., Schlessinger, K., Wegrzyn, J., Larner, A.C., and Levy, D.E. (2009). Mitochondrial STAT3 supports Ras-dependent oncogenic transformation. Science *324*, 1713–1716.

Gough, D.J., Marié, I.J., Lobry, C., Aifantis, I., and Levy, D.E. (2014). STAT3 supports experimental K-RasG12D-induced murine myeloproliferative neoplasms dependent on serine phosphorylation. Blood *124*, 2252–2261.

Guo, G., Huang, Y., Humphreys, P., Wang, X., and Smith, A. (2011). A PiggyBac-based recessive screening method to identify pluripotency regulators. PLoS ONE *6*, e18189.

He, J., Mao, C.-C., Reyes, A., Sembongi, H., Di Re, M., Granycome, C., Clippingdale, A.B., Fearnley, I.M., Harbour, M., Robinson, A.J., et al. (2007). The AAA+ protein ATAD3 has displacement loop binding properties and is involved in mitochondrial nucleoid organization. J. Cell Biol. *176*, 141–146.

Houghton, F.D., Thompson, J.G., Kennedy, C.J., and Leese, H.J. (1996). Oxygen consumption

and energy metabolism of the early mouse embryo. Mol. Reprod. Dev. *44*, 476–485.

Khacho, M., Clark, A., Svoboda, D.S., Azzi, J., MacLaurin, J.G., Meghaizel, C., Sesaki, H., Lagace, D.C., Germain, M., Harper, M.-E., et al. (2016). Mitochondrial Dynamics Impacts Stem Cell Identity and Fate Decisions by Regulating a Nuclear Transcriptional Program. Cell Stem Cell *19*, 232–247.

Kunath, T., Saba-El-Leil, M.K., Almousailleakh, M., Wray, J., Meloche, S., and Smith, A. (2007). FGF stimulation of the Erk1/2 signalling cascade triggers transition of pluripotent embryonic stem cells from self-renewal to lineage commitment. Development *134*, 2895–2902.

Lapuente-Brun, E., Moreno-Loshuertos, R., Acín-Pérez, R., Latorre-Pellicer, A., Colás, C., Balsa, E., Perales-Clemente, E., Quirós, P.M., Calvo, E., Rodríguez-Hernández, M.A., et al. (2013). Supercomplex assembly determines electron flux in the mitochondrial electron transport chain. Science *340*, 1567–1570.

Lu, C., and Thompson, C.B. (2012). Metabolic regulation of epigenetics. Cell Metab. *16*, 9–17.

Lukas, J., Herzinger, T., Hansen, K., Moroni, M.C., Resnitzky, D., Helin, K., Reed, S.I., and Bartek, J. (1997). Cyclin E-induced S phase without activation of the pRb/E2F pathway. Genes Dev. *11*, 1479–1492.

Macias, E., Rao, D., Carbajal, S., Kiguchi, K., and DiGiovanni, J. (2014). Stat3 binds to mtDNA and regulates mitochondrial gene expression in keratinocytes. J. Invest. Dermatol. *134*, 1971–1980.

Martello, G., Bertone, P., and Smith, A. (2013). Identification of the missing pluripotency mediator downstream of leukaemia inhibitory factor. Embo J. *32*, 2561–2574.

Martello, G., Sugimoto, T., Diamanti, E., Joshi, A., Hannah, R., Ohtsuka, S., Göttgens, B., Niwa, H., and Smith, A. (2012). Esrrb is a pivotal target of the Gsk3/Tcf3 axis regulating embryonic stem cell self-renewal. Cell Stem Cell *11*, 491–504.

Masui, S., Nakatake, Y., Toyooka, Y., Shimosato, D., Yagi, R., Takahashi, K., Okochi, H., Okuda, A., Matoba, R., Sharov, A.A., et al. (2007). Pluripotency governed by Sox2 via regulation of Oct3/4 expression in mouse embryonic stem cells. Nat. Cell Biol. *9*, 625–635.

Mathieu, J., and Ruohola-Baker, H. (2017). Metabolic remodeling during the loss and acquisition of pluripotency. Development *144*, 541–551.

Meier, J.A., and Larner, A.C. (2014). Toward a new STATe: the role of STATs in mitochondrial function. Semin. Immunol. *26*, 20–28.

Nichols, J., Zevnik, B., Anastassiadis, K., Niwa, H., Klewe-Nebenius, D., Chambers, I., Schöler, H., and Smith, A. (1998). Formation of pluripotent stem cells in the mammalian embryo depends on the POU transcription factor Oct4. Cell *95*, 379–391.

Nichols, J., and Smith, A. (2012). Pluripotency in the embryo and in culture. Cold Spring Harb Perspect Biol *4*, a008128–a008128.

Niwa, H., Burdon, T., Chambers, I., and Smith, A. (1998). Self-renewal of pluripotent embryonic stem cells is mediated via activation of STAT3. Genes Dev. *12*, 2048–2060.

Pardo, M., Lang, B., Yu, L., Prosser, H., Bradley, A., Babu, M.M., and Choudhary, J. (2010). An expanded Oct4 interaction network: implications for stem cell biology, development, and disease. Cell Stem Cell *6*, 382–395.

Pereira, L., Yi, F., and Merrill, B.J. (2006). Repression of Nanog gene transcription by Tcf3 limits embryonic stem cell self-renewal. Mol. Cell. Biol. *26*, 7479–7491.

Sánchez-Castillo, M., Ruau, D., Wilkinson, A.C., Ng, F.S.L., Hannah, R., Diamanti, E., Lombard, P., Wilson, N.K., and Göttgens, B. (2015). CODEX: a next-generation sequencing experiment database for the haematopoietic and embryonic stem cell communities. Nucleic Acids Res. *43*, D1117–D1123.

Schöler, H.R., Dressler, G.R., Balling, R., Rohdewohld, H., and Gruss, P. (1990). Oct-4: a germline-specific transcription factor mapping to the mouse t-complex. Embo J. *9*, 2185–2195.

Sieber, M.H., Thomsen, M.B., and Spradling, A.C. (2016). Electron Transport Chain Remodeling by GSK3 during Oogenesis Connects Nutrient State to Reproduction. Cell *164*, 420–432.

Smith, A.G. (2001). Embryo-derived stem cells: of mice and men. Annu. Rev. Cell Dev. Biol. *17*, 435–462.

Smith, A.G., Heath, J.K., Donaldson, D.D., Wong, G.G., Moreau, J., Stahl, M., and Rogers, D. (1988). Inhibition of pluripotential embryonic stem cell differentiation by purified polypeptides. Nature *336*, 688–690.

Srivastava, J., and DiGiovanni, J. (2016). Non-canonical Stat3 signaling in cancer. Mol. Carcinog. *55*, 1889–1898.

Szczepanek, K., Chen, Q., Derecka, M., Salloum, F.N., Zhang, Q., Szelag, M., Cichy, J., Kukreja, R.C., Dulak, J., Lesnefsky, E.J., et al. (2011). Mitochondrial-targeted Signal transducer and activator of transcription 3 (STAT3) protects against ischemia-induced changes in the electron transport chain and the generation of reactive oxygen species. J. Biol. Chem. *286*, 29610–29620.

Szczepanek, K., Xu, A., Hu, Y., Thompson, J., He, J., Larner, A.C., Salloum, F.N., Chen, Q., and Lesnefsky, E.J. (2015). Cardioprotective function of mitochondrial-targeted and transcriptionally inactive STAT3 against ischemia and reperfusion injury. Basic Res. Cardiol. *110*, 53.

Tammineni, P., Anugula, C., Mohammed, F., Anjaneyulu, M., Larner, A.C., and Sepuri, N.B.V. (2013). The import of the transcription factor STAT3 into mitochondria depends on GRIM-19, a component of the electron transport chain. J. Biol. Chem. *288*, 4723–4732.

Warburg, O., Wind, F., and Negelein, E. (1927). THE METABOLISM OF TUMORS IN THE BODY. J. Gen. Physiol. *8*, 519–530.

Ward, B.L., Anderson, R.S., and Bendich, A.J. (1981). The mitochondrial genome is large and variable in a family of plants (cucurbitaceae). Cell *25*, 793–803.

Wegrzyn, J., Potla, R., Chwae, Y.-J., Sepuri, N.B.V., Zhang, Q., Koeck, T., Derecka, M., Szczepanek, K., Szelag, M., Gornicka, A., et al. (2009). Function of mitochondrial Stat3 in cellular respiration. Science *323*, 793–797.

Wiesner, R.J., Rüegg, J.C., and Morano, I. (1992). Counting target molecules by exponential polymerase chain reaction: copy number of mitochondrial DNA in rat tissues. Biochem. Biophys. Res. Commun. *183*, 553–559.

Wray, J., and Hartmann, C. (2012). WNTing embryonic stem cells. Trends Cell Biol. *22*, 159–168.

Yi, F., Pereira, L., Hoffman, J.A., Shy, B.R., Yuen, C.M., Liu, D.R., and Merrill, B.J. (2011). Opposing effects of Tcf3 and Tcf1 control Wnt stimulation of embryonic stem cell self-renewal. Nat. Cell Biol. *13*, 762–770.

Ying, Q.-L., Wray, J., Nichols, J., Batlle-Morera, L., Doble, B., Woodgett, J., Cohen, P., and Smith, A. (2008). The ground state of embryonic stem cell self-renewal. Nature *453*, 519–523.

Yoshida, K., Chambers, I., Nichols, J., Smith, A., Saito, M., Yasukawa, K., Shoyab, M., Taga, T., and Kishimoto, T. (1994). Maintenance of the pluripotential phenotype of embryonic stem cells through direct activation of gp130 signalling pathways. Mech. Dev. *45*, 163–171.

Zhang, J., Ratanasirintrawoot, S., Chandrasekaran, S., Wu, Z., Ficarro, S.B., Yu, C., Ross, C.A., Cacchiarelli, D., Xia, Q., Seligson, M., et al. (2016). LIN28 Regulates Stem Cell Metabolism and Conversion to Primed Pluripotency. Cell Stem Cell *19*, 66–80.

Zhou, W., Choi, M., Margineantu, D., Margaretha, L., Hesson, J., Cavanaugh, C., Blau, C.A., Horwitz, M.S., Hockenbery, D., Ware, C., et al. (2012). HIF1α induced switch from bivalent to exclusively glycolytic metabolism during ESC-to-EpiSC/hESC transition. Embo J. *31*, 2103–2116.

Al termine di questi tre anni di Dottorato desidero ringraziare tutte le persone che in un modo o nell'altro mi hanno aiutato a portare a termine questo non facile percorso:

In primo luogo ringrazio i miei supervisori Graziano Martello e Elena Carbognin per avermi dato i giusti consigli e i giusti strumenti per superare le varie difficoltà trovate durante questi tre anni.

Un ringraziamento a tutti i colleghi di laboratorio con cui ho condiviso momenti di sconforto e di gioia, e che in un modo o nell'altro mi hanno aiutato e sostenuto sia da un punto di vista sperimentale che morale.

Un ringraziamento speciale va a tutta la mia famiglia che mi ha sostenuto e ha reso possibile questo percorso di studi culminato nella scrittura di questa Tesi.

Infine vorrei ringraziare Martina Castellan la persona a me più vicina e con la quale ho condiviso gioie e dolori durante tutto il periodo universitario. Senza la quale non avrei affrontato con la stessa energia e tranquillità questo lungo e tortuoso percorso.

Ringrazio alla fine anche me stesso per aver dimostrato ancora una volta di essere in grado di mantenere gli impegni presi e di portare a termine il percorso scelto nonostante le difficoltà.